Master's Thesis
Aalborg University, 2015

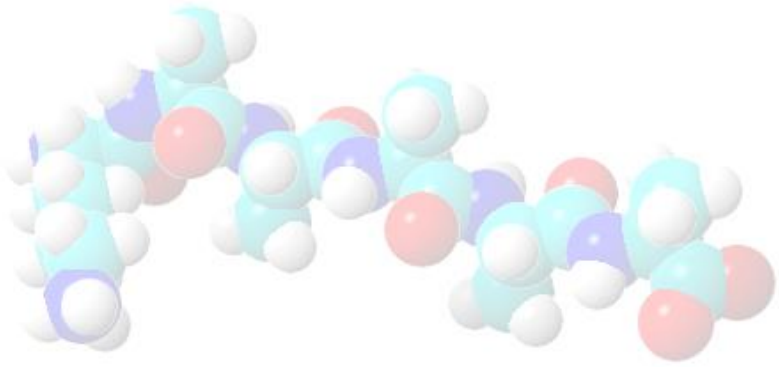

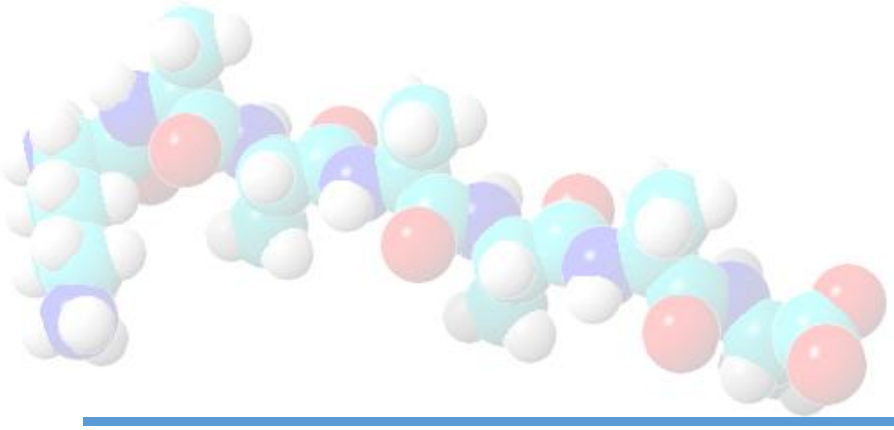

Investigation of the Self-assembling Properties of the Peptide KA_5 Family

Ruben Peter Eeg

Aalborg University

Department of Physics and Nanotechnology

Title:

Investigation of the self-assembling properties of the peptide KA_5

Project Period:

September 1st, 2014 - September 15th, 2015

Author:

Ruben Peter Eeg

Supervisors:

Leonid Gurevich

Peter Fojan

Abstract:

This report investigates the self-assembly of the KA_5 family of peptides. Theory behind the self-assembly of surfactants were described, together with examples of self-assembly by surfactant-like peptides. Furthermore the solid-phase peptide synthesis together with the force field simulations are described.

The KA_5 family of peptides were synthesized. After the synthesis the peptides were purified through HPLC before being washed with HCl. Structures were formed through self-assembly and imaged with AFM. The structures formed in vitro were compared to structures formed in silico.

Number of appendices: 1

Total number of pages: 79

Number of reports printed: 4

Dansk Abstract

Denne rapport undersøger selv-organisering af peptidet KA_5 og lignende peptider. Teorien omkring selv-organisering af surfactanter er beskrevet sammen med exempler på selv-organisering af surfactant lignende peptider. Endvidere beskrives solid-phase peptide synthesis og force field simuleringer.

KA_5 og lignene peptider blev syntetiseret. Efter syntesen blev peptiderne oprenset igennem HPLC før de blev vasket med HCl. Structure blev dannet igennem selv-organisering og afbilledet med AFM. Strukturerne dannet in vitro blev sammenlignet med strukture dannet in silico.

PREFACE

This report is produced by a nanotechnology student on the 5^{th} year at Aalborg University. The report was produced in the period of 1^{st} of September 2015 to 15^{th} of September 2015.

Reading Guide

Throughout the report, there will be references to various sources. These will be found on the form [#] where the number in the angular brackets refers to a specific source in the bibliography at the end of the report. In the bibliography the sources will be listed with its title, author, and other relevant information depending on whether the source is a book, article, or web page. The bibliographic references will be listed after the specific section in which they are used; this indicates that the reference applies to all of the above if nothing else is stated.

Tables and figures are listed after the number of the chapter in which they are displayed. Hence the first figure in chapter 4 would be named 'Figure 4.1' whereas the next one would be 'Figure 4.2' et cetera. Since tables are numbered according to the same system both 'Table 4.1' and 'Figure 4.1' are possible in the same chapter. To each figure/table a short descriptive caption will be made together with a bibliographic reference where necessary. All figures can be found on the attached CD.

The front page illustrates KA_4, KA_5, and KA_6.

Ruben Vitting-Eeg

CONTENTS

CHAPTER 1

INTRODUCTION

1.1 Self-assembly of Surfactant-like Peptides

Mankind has always sought for a high quality of life and a long lifespan. This has through many years led to the medicine we know and use today. This search is bringing researchers into the field of bionanotechnology. Bionanotechnology is a new scientific field and over the past decades the field has gone from creating novel nanostructures to finding and using their potential. Many different nanostructures has been created including, carbon nanotubes, nanoparticles, and self-assembled micelles and vesicles. These structures have been evaluated in disease diagnostics, drug delivery, and wound healing, among others. The first medicine, that made use of nanotechnology is from 2005, an anticancer drug called taxol. In this case taxol was loaded into protein nanoparticles, this resulted in the treatment being more effective towards cancer cells and less toxic for the patient. [1] [2] [3]

Efficient medicines are created to suit a specific medical purpose, which requires functional and structural control. One way to achieve this is through self-assembly. Self-assembly allows control over the synthesis of bioactive structures that can have variable size, shape and surface chemistry. The production of a variety of nanostructures is still only practically possible with self-assembly. Self-assembly is driven by free energy, which causes the molecules to spontaneously organize themselves. The force that drives molecular self-assembly is usually not covalent bonds but ionic bonds, hydrophobic and hydrophilic interactions, van der Waals, or hydrogen bonds. This can lead to the molecules aggregating spontaneously into ordered structures. [1] [2] [3] [4]

To produce self-assembled structures, building blocks are needed. One material that has been proven useful as building blocks for medical self-assembly are peptides. One reason for peptides being useful is their biodegradability, which can be tuned by using specific sequences of amino acids, and their biocompatibility. Peptides provide a great platform

for self-assembly and design of nanostructures because of their ability to adopt secondary structures as well as being chemically versatile. Oligopeptides can be synthesized with ease through solid-phase synthesis, however it is still a challenge to synthesize large proteins with hundreds of amino acids. The goal with using self-assembling of peptides in medicine is to create nanoscale biomaterials where the functionality of peptides is combined with their versatile structures. [1] [2] [4]

There are four categories in peptide based self-assembly, these being: coiled-coils, β-sheets, β-hairpins, and surfactant-like peptides. Surfactant-like peptides are the ones primarily used for drug delivery. One reason for this is that coiled-coils, β-sheets, and β-hairpins usually create nanofibers through self-assembly, but surfactant-like peptides can be designed in such a way that they will self-assemble into micelles with a hydrophilic surface and hydrophobic center, this structure among others are illustrated by Figure 1.1. Self-assembled structures, e.g. micelles, inverted micelles, or vesicle, created with amphiphiles can transform into each other if the environment is changed. [2] [5] [6]

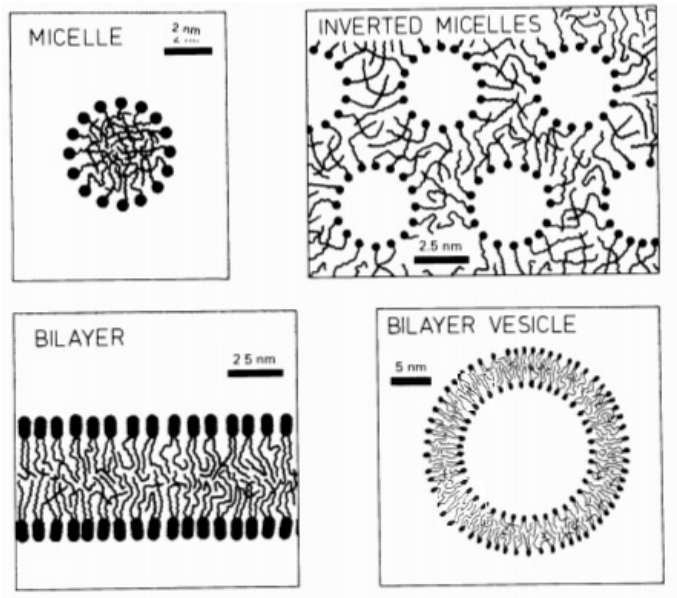

Figure 1.1: Illustration of micelles, inverted micelles, bilayer, and bilayer vesicle created with amphiphiles. [5]

The surfactant-like peptide may have a hydrophilic headgroup and a hydrophobic tail, where the headgroup is made from at least one polar amino acid, lysine, arginine, or histidine for a positive charged headgroup, while aspartic and glutamic acid can be used for a negatively charged headgroup, while the tail is made from nonpolar amino acids e.g. alanine, valine, or leucine. [6] [7]
The changes of the tail residues of the surfactant-like peptide may affect the intermolecular interactions and thereby the packing of the peptide may be changed. Furthermore the charges

of the hydrophilic headgroup may have an influence of the self-assembled structures formed, as they will increase the ionic repulsion. [5] [8] This influence is described by Israelachvili et al. [9]

Self-assembled aggregates will not form unless the concentration of surfactants are above the critical aggregation concentration, CAC, or critical micelle concentration, CMC, which is more conventional term. As long as the concentration of surfactants are below CMC only monomers will be present in the solution. When the concentration of surfactant reaches CMC it cannot increase further and aggregates will start to form, illustrated by Figure 1.2. [5]

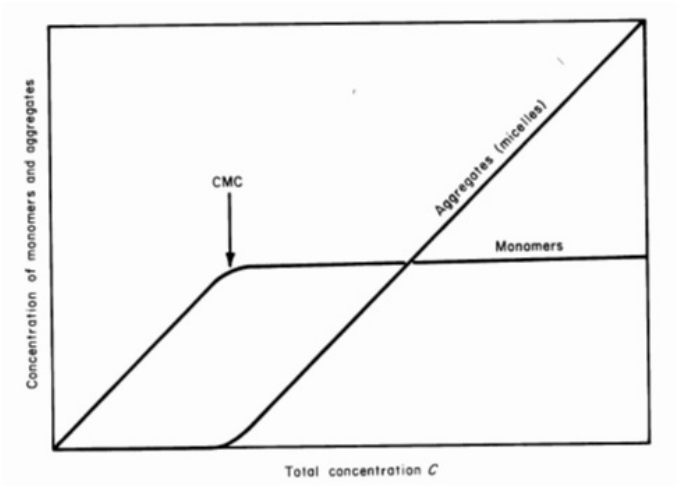

Figure 1.2: Graph illustrating the concentration of aggregates and monomers as a function of the concentration of surfactant. CMC is noted where the concentration of monomers cannot increase further and the aggregates start to form. [5]

The aggregates created through self-assembly can be within a wide range of structures, e.g. small spherical micelles, long cylindrical micelles, and bilayers. The structure of self-assembled micelles can be described by the volume, v, divided by the cross-sectional area of the hydrophilic headgroup, a, and the molecular length, l, $\frac{v}{a \cdot l}$. The critical condition for the formation of spheres is $\frac{v}{a \cdot l} = \frac{1}{3}$, and if $\frac{v}{a \cdot l} > \frac{1}{3}$ spherical micelles cannot form, however non-spherical micelles may form. For cylindrical micelles the critical condition is $\frac{v}{a \cdot l} = \frac{1}{2}$, while $\frac{v}{a \cdot l} = 1$ is the critical condition for planar bilayers. However these are only the case if it is assumed, that the surface area of each surfactant is equal or close to the optimal area. [9]

The structural features of the product can be finely tuned by varying the environment of the reaction, e.g. pH, temperature, or solvent. These can be manipulated to achieve the desired function, which may not necessarily be thermodynamically stable structures. The desired structures may be structures that can maintain their structure and function within a certain environment or a desired timescale. An example of this is that most tumors are intracellular acidic with a pH less than 6, however normal tissue has a pH of 7.4. This knowledge can be used to design smart drug carriers which can respond to a pH change and

thereby have a potential use in anti-tumor drug delivery. [1] [2] [3]

1.1.1 Phospholipid-like Peptides

With inspiration from lipids found in Nature Zhao et al. designed lipid-like self-assembling peptides in 2006. [10]
Lipid-like peptides were designed with hydrophilic head and hydrophobic tails so they would form structures in H_2O. The peptides designed had heads consisting of either a positively charged lysine or a negatively charged aspartic acid. The tails consisted of alanine, valine, or leucine. The peptides contained 7 or 8 amino acids to have similar lengths to phospholipids, ~2.5 nm. It was found that these peptides formed ordered structures. Furthermore it was found that the peptides had distinct critical aggregation concentrations. [10]
It was attempted to mimic the phospholipids even further by using alanine or valine as the hydrophobic tail while using the artificial amino acid, phosphoserine as the hydrophilic head. It was found that these peptides, similar to the peptides with natural amino acids, had critical aggregation concentrations and form well ordered structures. [10]

It was found that the peptides formed nanotubes and nanovesicles with average diameter between 30 nm and 50 nm when the peptides were self-assembling in H_2O. The peptides where the tails consisted of alanine or valine was found to form more stable and homogeneous structures, when compared to the structures formed by peptides with tails consisting of glycine, isoleucine, or leucine. And it was suggested that if the chemical properties and self-assembling behaviour were to be fully understood, it would be possible to build materials from the bottom up. [10]

1.1.2 Peptides $\mathbf{A_6/V_6/L_6D}_n$

One family of surfactant-like peptides that has self-assembling properties is peptides containing one or two aspartic acids at the C-terminus, which leads to two or three negative charges on the hydrophilic headgroup. The hydrophobic tails of these peptides consists of six alanine, leucine or valine. The N-terminus is acetylated to eliminate the positive charge. This family of surfactant-like peptides were investigated by Vauthey et al. in 2001.[8] Aspartic acid is negative charged at neutral pH but is protonated and uncharged in solutions below pH 3.5. [8]

There is a fine balance between charge and hydrophobic residues if the surfactant-like peptides have to be soluble in water. If there is too many hydrophobic residues the peptide can become insoluble, and if the peptide has too many charges the peptide may become too soluble and the electrostatic interactions may cause repulsion. [8]

Vauthey et al. found that the structures formed by A_6D (A), V_6D (B) and V_6D_2 (C) were similar but varied in size, however L_6D_2 (D) formed quite different structures, Figure 1.3. This indicates that the packing of the hydrophobic tail may differ based on the size of the residues. The self-assembled structures formed are dense networks consisting of tubes with

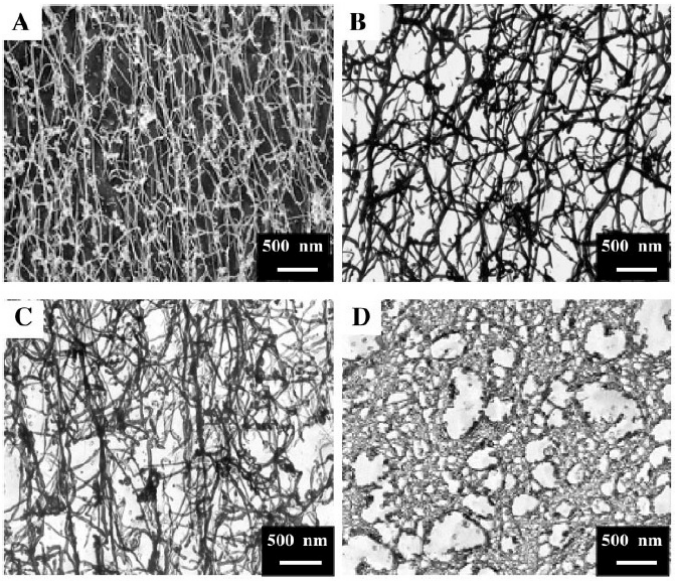

Figure 1.3: Quick-freeze/deep-etch TEM images of self-assembled networks formed by 4.3 mM A_6D (A), V_6D (B), V_6D_2 (C), and L_6D_2 (D) in H_2O. The diameter of the tubes that form the net is ~30-50 nm and lengths of tens of micrometers. The images seem more dense than the actual structures in the solutions since the solution has structures in 3D while the imaged is in 2D. [8]

diameter between 30 nm and 50 nm with lengths up to tens of micrometers and vesicles with similar diameter. The network is formed by three-way junctions connecting the tubes and thereby forming the network. A potential pathway of the self-assembly forming V_6D tubes is illustrated by Figure 1.4. The potential pathway starts with monomers self-assembling into closed rings, these closed rings can then stack on top of each other to form tubes. Three tubes can then connect through a three-way junction. [8]

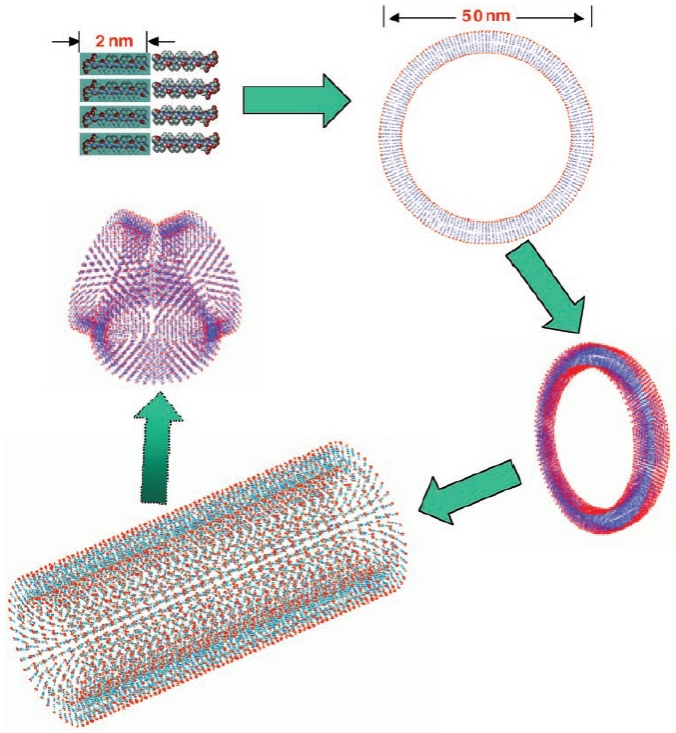

Figure 1.4: Illustration of a potential pathway for formation of V_6D nanotubes and three-way junctions. The hydrophilic headgroups are marked with red and the hydrophobic tails are marked with blue. V_6D monomers with lengths of 2 nm may interact with each other and form closed rings with diameters of 50 nm, these can stack and form tubes. Finally three tubes can then connect and form three way junctions. [8]

1.1.3 Peptides G_nD_2

Experiments has also been done with a similar family of peptides. This family has four to ten glycine at the N-terminus end as the hydrophobic tail and two aspartic acids at the C-terminus end as the hydrophilic headgroup. Santoso et al. found that the solubility of the peptide decreased when the length of the tail was increased, and peptides with tails longer than ten glycines were not investigated due to this. [11]

The structures were investigated by dynamic light scattering, where it was found that structures were formed and that the dimensions of the structures were 40-80 nm. It was also found that G_6D_2 formed structures with sizes of 100 to 200 nm. These peaks from the dynamic light scattering experiment became more prominent when the length of the tail was increased, This distribution can be seen on Figure 1.5. It was found that longer tails resulted in a broader size distribution due to increased flexibility of the longer tails. The lenghts of potential nanotubes were not measured due to the instrument was limited to sizes between 10 to 1000 nm. [11]

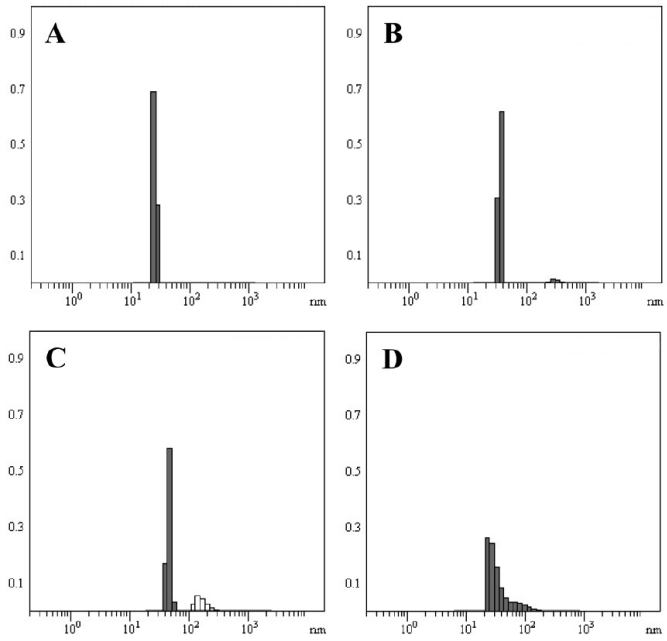

Figure 1.5: Size distribution of structures formed with G_nD_2 measured with dynamic light scattering, A is G_4D_2, B is G_6D_2, C is G_8D_2, D is $G_{10}D_2$. The length of nanotubes is not measured due to the instrument was only able to measure lengths between 10 and 1000 nm. [11]

TEM was used to detect structures that could not be detected by dynamic light scattering. Quick-freeze/deep-etch was used to prepare the samples for TEM to preserve the structures formed in solution. It was found that G_4D_2 formed mainly nanotubes with diameter at roughly 40 nm along with a small amount of vesicles. G_6D_2 was found to form similar nanotubes, but more vesicles than G_4D_2. Both G_8D_2 and $G_{10}D_2$ was found to form nanotubes. The nanotubes formed by G_8D_2 and $G_{10}D_2$ were more entangled than the nanotubes formed by G_4D_2 and G_6D_2. The TEM images can be seen on Figure 1.6. [11]

With increasing amount of residues in the glycine tail the monomers could be packed closely and thereby form membranes with thickness of around 10 nm. The thickness of the bilayer could vary depending on how the monomers will overlap in the bilayer. Membranes could sustain a low curvature and thereby prevent the formation of vesicles and tubes. [11]

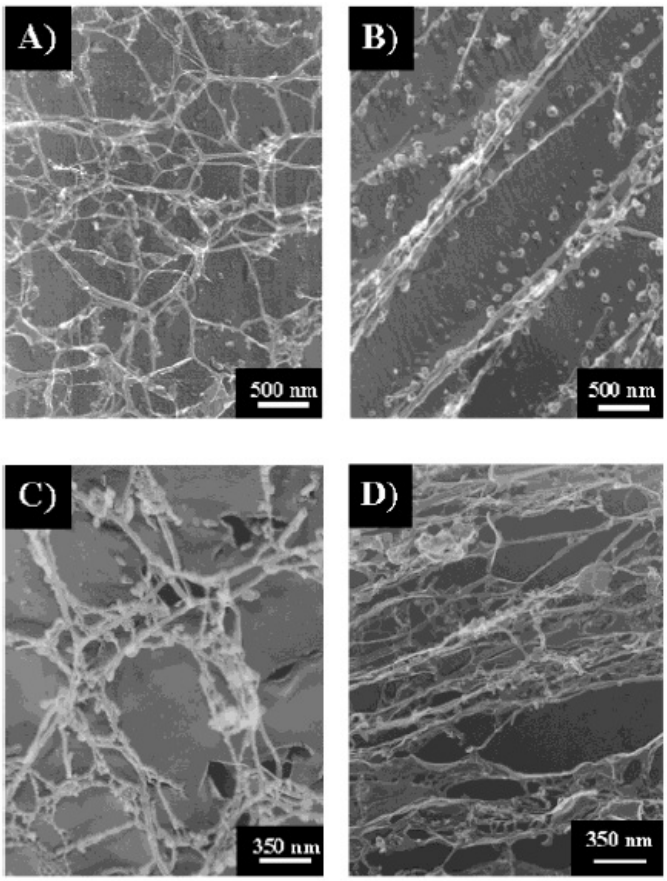

Figure 1.6: TEM images of quick-freeze/deep-etch G_nD_2, where A is G_4D_2, B is G_6D_2, C is G_8D_2, D is $G_{10}D_2$. All four TEM images has nanotubes with diameter of the nanotubes is around 40 nm. G_6D_2 also formed vesicles with diameter similar to the nanotubes. [11]

1.2 Solid-phase Peptide Synthesis

Many uses for peptides exists in biology and biomedicine among others, for this reason the easiest and fastest way to obtain peptides is desired. Peptides can be chemically synthesized with ease unlike proteins, which are generally produced by recombinant methods. The most common method to produce peptides chemically is through solid-phase peptide synthesis, SPPS. Proteins are often produced via recombinant methods, while peptides can be produced through chemical synthesis with ease. [12]

In the 1960s an idea that solid support could anchor the amino acids allowed for a revolution in the field of peptide science and SPPS was introduced. Since the 1960s SPPS has been developed further and the method has been evolved into an efficient technique to synthesize peptides, and the method may even be used for synthesis of small proteins. Even though the method is called Solid-Phase Peptide synthesis, a better name for the method would be Matrix Assisted Peptide Synthesis, as the resin used is far from solid. The reason for

using a matrix for the synthesis is that the first amino acid or an amino group is immobilized on the matrix, this allows for the amino acid to be filtered. This also allows the solution in which the synthesis has happened to be washed and the peptide can be released from the matrix. [12]

An amino acid has two functional groups, an amino group and an acid group, this can cause unintended reactions and thereby creating unintended products. Because of this, the amino group from one amino acid and the carboxyl group of the second amino acid has to be protected to ensure the right peptide bond is made. Some amino acids also require additional protection groups because of additional functional groups e.g. the amino group on lysine or the carboxyl group on glutamic acid. One way to protect the amino group is with a carboxybenzyl, while the carboxyl group could be protected as a benzyl ester, which will allow coupling of the two amino acids and form the peptide bond. This process can be continued and thereby form a peptide longer than two amino acids. The method can also be used to couple two peptides together. The binding of two amino acids with protection groups is illustrated by Figure 1.7. [12]

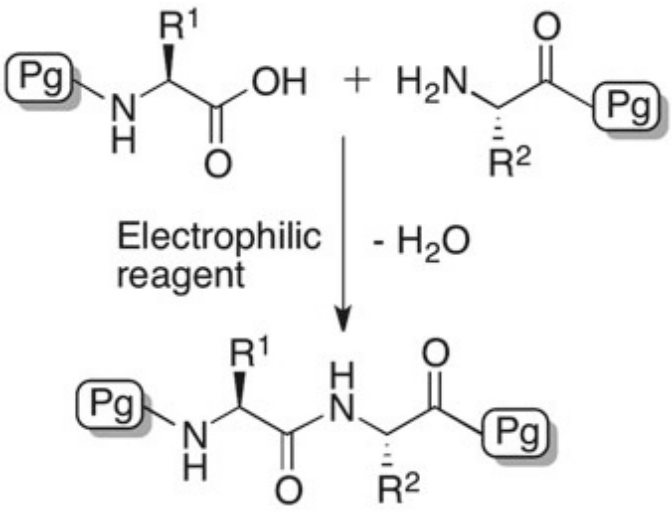

Figure 1.7: Synthesis of a peptide bond, where Pg are the protection groups preventing active groups from reacting. [12]

Two protection groups are dominant in SPPS one being fluoren-9-ylmethyloxycarbonyl, Fmoc, and the other being tert-butoxycarbonyl, Boc. Each protection group define the chemical window in the SPPS, and thereby the method is defined by the protection group used. For SPPS where Fmoc is used as protection group the Fmoc protection group is removed and the amino acid deprotected with 20% piperidine in DMF. The release of the peptide from the support is often based on trifluoroacetic acid, TFA. For SPPS with Boc protection groups TFA is used for removal of Boc protection groups while the release of the peptide from the

support is often done with hydrofluoric acid, HF. [12]

Before an carboxylic acid of one amino acid can react with the Nα-amino group, the carboxylic acid has to be activated. The first step of the activation is having the carboxylic acid react with an electrophile. During the activation, side reactions may occur, which can cause an O-to-N rearrangement of the O-acylisourea intermediate, this will overactivate the carboxylic acid. The overactivation may lead to epimerization illustrated by Figure 1.8. [12]

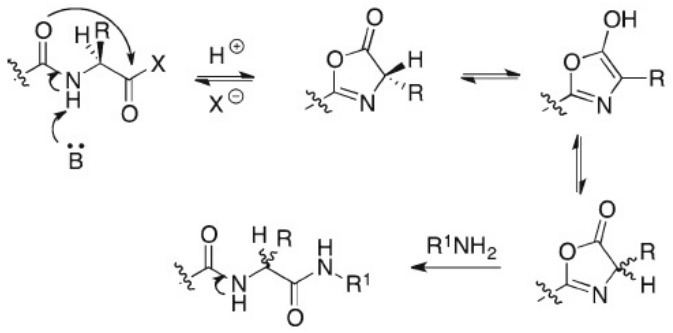

Figure 1.8: Illustration of how overactivation of the carboxylic acid can change the chirality of an amino acid. [12]

Side reactions can be prevented and one way to prevent them is by addition of auxiliary nucleophiles e.g. ethyl 2-cyano-2-(hydroxyimino)acetate, Oxyma. When auxiliary nucleophiles are present activated, esters will be formed which ensures that the chirality of the activated amino acid is maintained. During the SPPS an in situ coupling reagents may also be used, an example and one of the most important ones is HBTU, N-[(1 H-benzotriazol-1-yl)(dimethylamino)methylene]-N-methylmethanaminium hexafluorophosphate N-oxide. These reduce coupling time and help to minimize epimerization. [12]

The first amino acid has to be immobilized on resins, in most cases the peptide chain is bound to the resin through a linker between the resin and the first amino acid. The most commonly used resins are based on polystyrene. Benefits with polystyrene is that it is cheap and works especially well in Boc-SPPS and shorter sequences of Fmoc-SPPS, however other resins exists if polystyrene does not fit the needs, an example of these is resins based on polyethylene glycol, PEG. [12]
The linker is a molecule has one end binding to the first amino acid, most commonly through the C-terminus, and one end that anchors it to the resin. This immobilizes the amino acids on the resin during the SPPS and allows release of the synthesized peptide when exposed to specific conditions. In Fmoc-SPPS most linkers release the peptide by acidolysis, most commonly done with solutions containing TFA. Most peptides are soluble in TFA, this allows for the peptide to be dissolved in TFA, which are then easily evaporated and the peptide can be isolated. [12]

1.3 Force Field Simulation

Molecular simulations may be required to simulate a system containing a large number of particles, as quantum mechanics may not be enough. Even if a couple of electrons can be ignored the calculations with quantum mechanics will need to describe nearly all particles, which will be complicated and time-consuming. One method that simplifies the system is the force field. The use of force fields ignore the motion of electrons and use only the nuclei positions to calculate the energies. This can lower the time required significantly, and may even provide results that is just as accurate as the calculations done with quantum mechanics. To use force fields for simulations it has to be assumed that the wavefunctions of the electrons and the nuclei can be separated, the Born-Oppenheimer approximation. [13]

The energy of each nucleus can be split into five components. The first part is the energy of the bond, which is described by a stretching constant, k, the bond length, l, and the equilibrium length of the bond, l_0, $v(l) = \frac{k}{2}(l-l_0)^2$. The second part is the energy of the angles, described by a force constant, k, the angle, θ, and an equilibrium angle, θ_0, $v(\theta) = \frac{k}{2}(\theta-\theta_0)^2$. The third part describes the torsion energy described by an energy barrier, V_n, the multiplicity, n, the torsion angle, ω, and the phase factor, γ, $V(\omega) = \sum_{n=0}^{N} \frac{V_n}{2}[1+cos(n\omega-\gamma)]$. [13]
The last two components is the non-bonded interactions. These are the electrostatic interactions and van der Waals interactions. The energy of the electrostatic interactions can be described by the charges of the two particles interacting, q_i and q_j, the permittivity, ϵ_0, and the distance between the charges, r_{ij}, $V = \sum_{i=1}^{N_A}\sum_{j=1}^{N_B} \frac{q_i q_j}{4\pi\epsilon_0 r_{ij}}$. The van der Waals interactions are split into two parts, an attractive part and a repulsive part, these can be described by a collision diameter, σ, the depth of the potential energy well, ϵ and the distance between the particles, r, $V(r) = 4\epsilon\left[\left(\frac{\sigma}{r}\right)^{12} - \left(\frac{\sigma}{r}\right)^{6}\right]$. These five equations, describing the five interactions illustrated by Figure 1.9, can be combined into a single equation describing the force field simulations. [13]

$$V(r^N) = \sum_{bonds} \frac{k_i}{2}(l_i - l_{i,0})^2 + \sum_{angles} \frac{k_i}{2}(\theta_i - \theta_{i,0})^2 + \sum_{torsions} \frac{V_n}{2}[1+cos(n\omega-\gamma)]$$
$$+ \sum_{i=1}^{N}\sum_{j=i+1}^{N}\left(\frac{q_i q_j}{4\pi\epsilon_0 r_{ij}} + 4\epsilon_{ij}\left[\left(\frac{\sigma_{ij}}{r_{ij}}\right)^{12} - \left(\frac{\sigma_{ij}}{r_{ij}}\right)^{6}\right]\right)$$

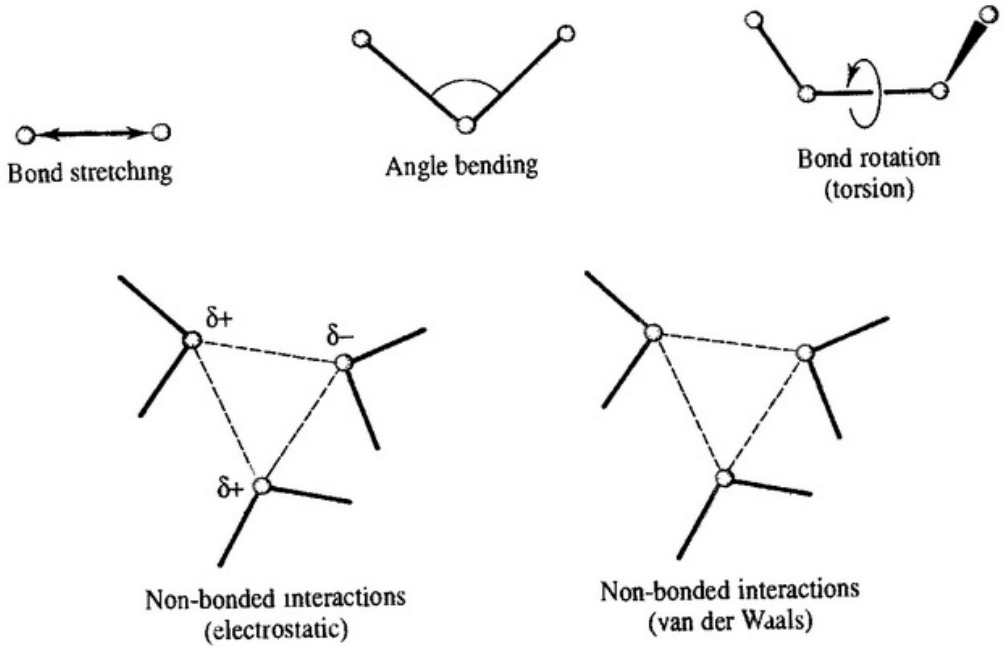

Figure 1.9: Illustration of the interactions used for force field simulations. The bond length and stretching, the angle bending, the rotation of bonds, and the non-bonded interactions van der Waals and electrostatic interactions. [13]

CHAPTER 2

EXPERIMENTAL PROCEDURES

2.1 Materials

Table 2.1 contains the chemicals used throughout the experiments.

Chemicals	
DIPEA	Iris (7087-68-5)
Trifluoroacetic acid	Iris (40320)
Acetonitril	Chemsolute (D3D058223D)
Dichloromethane	Iris (V0M992080N)
HBTU	Iris (110731)
OxymaPure	Iris (1106117001)
Piperidine	Iris (781841)
Dimethylformamide	Iris (D4F057014G)
Diethylether	Iris (V1l778141L)
TIS	Iris (0299552)
H_2O	In-house
HCl	Sigma-Aldrich (SZBE2740V)
NaOH	Bie & Berntsen (4228203)
Thioflavin-T	Sigma (MKBS6089)

Table 2.1: The table has a list of chemicals used throughout the practical work. The table contains the name of the chemical as well as the supplier and lot or batch number.

Table 2.2 contains the Columns used throughout the experiments. The Acclaim 300 C18 3 μm 300 Å will be referred to as the small column and the Gemini - NX 5 u C18 110 Å will be referred to as the large column.

HPLC Columns	
Acclaim 300 C18 3 μm 300 Å	Dionex (007-02-022)
Gemini - NX 5 u C18 110 Å	phenomenex (00G-4454-N0)

Table 2.2: The table contians the two columns used for HPLC.

Table 2.3 contains the amino acids and resins used throughout the experiments.

Amino acids and resins	
Fmoc-Lys(Boc)-OH	Advanced ChemTech (19763-2)
Fmoc-Ala-OH·H_2O	Advanced ChemTech (10F17-L101)
Fmoc-Rink-Amide MBHA Resin	Iris (2536)
Fmoc-L-Ala-Wang Resin	Matrix (10K08-20-08-0)

Table 2.3: The table has a list of amino acids and resins used throughout the practical work. The table contains the name of the amino acid or resin as well as the supplier and lot or batch number.

2.2 Methods

2.2.1 Solid-phase Peptide Synthesis

Fmoc-SPPS were used to synthesize the peptides used for experiments.

Non-amidated KA_5

The first peptide synthesized was the synthesis of non-amidated KA_5. For this synthesis the following amino acids were used.

Substance	Mass [mg]
Fmoc-L-Ala-Wang Resin	240
Fmoc-Ala-OH·H_2O	233
Fmoc-Ala-OH·H_2O	233
Fmoc-Ala-OH·H_2O	232
Fmoc-Ala-OH·H_2O	232
Fmoc-Lys(Boc)-OH	352

Furthermore the following solutions were required,

Solution	Volume [mL]
DCM	15.0
1.0 M Dipea in DMF	17.5
0.5 M HBTU and 0.5 M oxymapure in DMF	17.5
25% Piperidine in DMF	90.0
DMF	1500

1 M dipea in DMF were prepared by dissolving 12.92 g in DMF for a total volume of 100 mL. 0.5 M HBTU and 0.5 M oxymapure in DMF were prepared by dissolving 7.11 g oxymapure and 18.96 g HBTU in DMF for a total volume of 100 mL. 25% dipea in DMF were prepared by dissolving 25 mL dipea in DMF for a total volume of 100 mL.

Amidated KA_5

The second peptide synthesis were the synthesis of amidated KA_5. For this synthesis the following amino acids were used.

Substance	Mass [mg]
Fmoc-Rink-Amide MBHA Resin	271
Fmoc-Ala-OH·H_2O	237
Fmoc-Ala-OH·H_2O	239
Fmoc-Ala-OH·H_2O	234
Fmoc-Ala-OH·H_2O	232
Fmoc-Ala-OH·H_2O	236
Fmoc-Lys(Boc)-OH	354

Furthermore the following solutions were required,

Solution	Volume [mL]
DCM	15.0
1.0 M Dipea in DMF	21.0
0.5 M HBTU and 0.5 M oxymapure in DMF	21.0
25% Piperidine in DMF	105
DMF	1832

Enough 1 M dipea in DMF was leftover from the synthesis of non-amidated KA_5 and therefore the same solution could be used. 0.5 M HBTU and 0.5 M oxymapure in DMF were prepared by dissolving 7.13 g oxymapure and 19.00 g HBTU in DMF for a total volume of 100 mL. 25% dipea in DMF were prepared by dissolving 50 mL dipea in DMF for a total volume of 200 mL.

Non-amidated KA_4

The third peptide synthesized was the synthesis of non-amidated KA_4. For this synthesis the following amino acids were used.

Substance	Mass [mg]
Fmoc-L-Ala-Wang Resin	247
Fmoc-Ala-OH·H_2O	234
Fmoc-Ala-OH·H_2O	234
Fmoc-Ala-OH·H_2O	240
Fmoc-Lys(Boc)-OH	353

Furthermore the following solutions were required,

Solution	Volume [mL]
DCM	15.0
1.0 M Dipea in DMF	14.0
0.5 M HBTU and 0.5 M oxymapure in DMF	14.0
25% Piperidine in DMF	75.0
DMF	1227

1 M dipea in DMF were prepared by dissolving 12.90 g in DMF for a total volume of 100 mL. 0.5 M HBTU and 0.5 M oxymapure in DMF were prepared by dissolving 7.10 g oxymapure and 18.97 g HBTU in DMF for a total volume of 100 mL. 25% dipea in DMF were prepared by dissolving 50 mL dipea in DMF for a total volume of 200 mL.

The synthesis was interrupted at the third alanine, therefore a new vial with 235 mg Fmoc-Ala-OH·H_2O was prepared, and the synthesis was continued.

Non-amidated KA_6

The last peptide synthesized was the synthesis of non-amidated KA_6. For this synthesis the following amino acids were used.

Substance	Mass [mg]
Fmoc-L-Ala-Wang Resin	240
Fmoc-Ala-OH·H_2O	241
Fmoc-Ala-OH·H_2O	237
Fmoc-Ala-OH·H_2O	240
Fmoc-Ala-OH·H_2O	241
Fmoc-Ala-OH·H_2O	235
Fmoc-Lys(Boc)-OH	358

Furthermore the following solutions were required,

Solution	Volume [mL]
DCM	15.0
1.0 M Dipea in DMF	21.0
0.5 M HBTU and 0.5 M oxymapure in DMF	21.0
25% Piperidine in DMF	105.0
DMF	1773

All the required solutions were leftover from the synthesis of non-amidated KA_4, and the leftovers could be used for this synthesis.

The synthesis was interrupted at the fourth alanine, therefore a new vial with 243 mg Fmoc-Ala-OH·H_2O was prepared, and the synthesis was continued.

2.2.2 Cleavage from Resin

After completed SPPS the peptides has to be cleaved from the resin. The solutions and chemicals required for this were DCM, diethylether(-18 degrees), and a solution of 95% TFA, 2.5% TIS, 2.5% H_2O.

First the resin is washed with DCM, 2 mL DCM is added to the reactor and is swelled for 90 seconds. The DCM washing is done four times. Reactor with resin is placed in a vacuum desiccator for ~2 hours. When the reactor is dry ~2 mL of the TFA/TIS/H_2O solution is added to the reactor and swelled for ~2 hours, the dilute is collected and the peptide should be in the dilute. Another ~2 mL of the TFA/TIS/H_2O solution is added to the reactor and the reactor is swelled for a few minutes, the dilute is collected into the same vial. The resin should now be without any peptide.
The peptide, in ~4 mL TFA/TIS/H_2O, is mixed well with ~10 mL diethylether, and centrifuged for ten minutes at 1400 g, supernatant is discarded. The pellet is resuspended in ~10 mL diethylether and centrifuged for ten minutes at 1400 g and the supernatant is discarded, this step is done twice. The pellet is freeze-dried and the peptide can now be stored at -18 degrees.

2.2.3 HPLC Purification

Two solvents were used for the HPLC, ACN and a solution with 0.1% of TFA dissolved in H_2O. The concentrations noted is the concentrations of ACN, and the rest of the solution run through the column is the 0.1% TFA solution.

Two programs were used for HPLC purification of peptides, each program had a unique gradient, illustrated by Figure 2.1.
The first program, illustrated by Figure 2.1A, was used for most of the peptide purifications. This program is 10% ACN until 5 minutes into the run, then the concentration of ACN is increased by 2.5% per minute until 15 minutes into the run. When the concentration of ACN

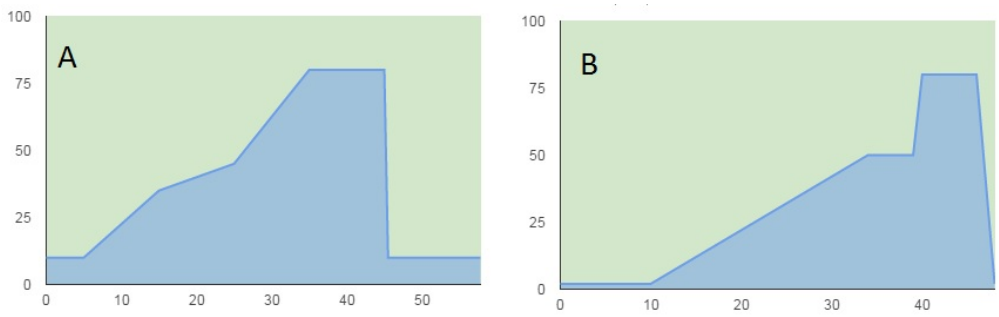

Figure 2.1: Illustrations of the two HPLC programs used throughout the practical work.

is 35% the increase is slowed to 0.5% per minute until 25 minutes after the program started. When the concentration of ACN is 45% the concentration is increased by 4% per minute until the concentration of ACN is 80%, after 35 minutes runtime, the 80% ACN is kept for 10 minutes, until minute 45. The concentration of ACN is lowered to 10% over the course of 30 seconds where it is kept stable until the program ends at 57.8 minutes.
The second program, illustrated by Figure 2.1B, was used for some HPLC runs where fractions were collected. This program started with an ACN concentration of 2% and was stable at 2% for 10 minutes. Then the concentration of ACN was increased by 2% per minute for 24 minutes, until 50% after 34 minutes runtime, and was stable for five minutes. The concentration was then increased by 30% per minute for one minute, for an ACN concentration of 80%, and was kept stable at 80% for six minutes until the runtime was 46 minutes. Lastly the ACN concentration was decreased to 2% over two minutes until 48 minutes runtime, where the program ended.

All peptides purified with HPLC was dissolved in H_2O containing 0.1% TFA.

2.2.4 Determination of Concentration

The concentrations of peptide was attempted to determine by measuring the absorbance at 205, and using Beer-Lambert law, $A_{205} = \epsilon_{205} cl$, where A_{205} is the absorbance at 205 nm, ϵ_{205} is the molar absorptivity at 205 nm, 31 $\frac{mL}{mg \cdot cm}$ is used, c is the concentration, and l is the length, 1 cm is used. [14]

2.2.5 HCl Purification

TFA could still be present after the HPLC purifications an freeze-drying of the peptide, therefore the peptides were washed with HCl.

The peptides were dissolved thoroughly in 10 mL of ~1M of HCl. The peptide solutions were freeze-dried to remove any liquid. The HCl wash was done twice to ensure optimum TFA removal.

2.2.6 Imaging of Structures

All imaging done with AFM is done on samples immobilized on mica. To obtain a range of pH values the pH of samples were adjusted towards lower pH with 0.1M and 1M HCl, and adjusted towards a higher pH with 0.1M and 1M NaOH. The pH is noted as acidic, neutral, or basic. Where acidic is noted the pH was below 4, where neutral is noted the pH was between 6 and 8, and where basic is noted the pH was above 10. After the pH adjustment the samples were exposed to ultrasound for five minutes to break down any structures formed before the pH adjustment. The solutions with peptide were left to self-assemble at 5°C. After the self-assembly ~20 μL were added to a mica surface and allowed to immobilize for 15-30 minutes and then blow-dried with nitrogen. Some samples were rinsed with ~2 mL H_2O and blow-dried again, if nothing is noted, the mica was not rinsed with H_2O after the immobilisation of structures.

2.2.7 Thioflavin-T

Experiments were done to investigate if the structures seen with AFM imaging were formed in the solution or formed on the mica surface. This investigation was done by having varying concentrations of thioflavin-T in the solution and measure the emission of thioflavin-T. The concentration of thioflavin-T in solutions with or without peptide varied from 0.5 μM to 50 μM.

CHAPTER 3

RESULTS

3.1 Amidated KA_5

3.1.1 HPLC Purification

Before any self-assembly was attempted with the amidated KA_5, the peptide was purified through HPLC. The peptide was run through the small column using the gradient illustrated by Figure 2.1A, resulting in the spectrum on Figure 3.1.

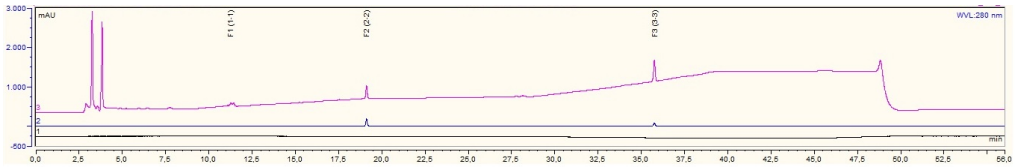

Figure 3.1: Spectrum a HPLC run of amidated KA_5, dissolved in 0.1% TFA in H_2O, where the small column and a 20 μL chamber is used. The dark blue line is the absorbance in mAU at 280 nm, the purple line is the absorbance in mAU at 220 nm, and the black line is the pump pressure in bar. Maximums were recognized based on the absorbance at 280 nm. The numbers above the maximums represents the vial in which a maximum was collected.

Three maximums were collected from the 20 μL sample and sent to be investigated with mass spectrometry. Meanwhile the rest of the peptide solution was run through the large column. This run, Figure 3.2B, yielded 42 maximums however only 41 were collected, maximum 4 was not collected by the HPLC program, a control run with 0.1% TFA dissolved in H_2O can be seen on Figure 3.2A.

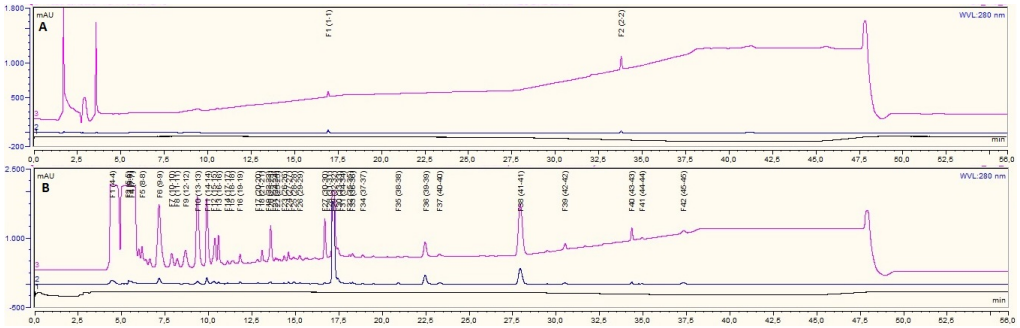

Figure 3.2: Spectres from two runs of HPLC where the large column and a 2 mL chamber is used. The dark blue line is the absorbance in mAU at 280 nm, the purple line is the absorbance in mAU at 220 nm, and the black line is the pump pressure in bar. maximums were recognized based on the absorbance at 280 nm. The numbers above the maximums represents the vial in which a maximum was collected. A is the spectrum of a HPLC run with pure 0.1% TFA dissolved in H_2O, control and B is the spectrum of a run where the synthesized amidated KA_5 is dissolved in the control solution, 0.1% TFA dissolved in H_2O.

After these runs the HPLC program was changed to recognize maximums based on the absorbance at 220 nm instead of 280 nm.

3.1.2 Self-assembly

After the HPLC purification the peptide was used for self-assembly experiments.

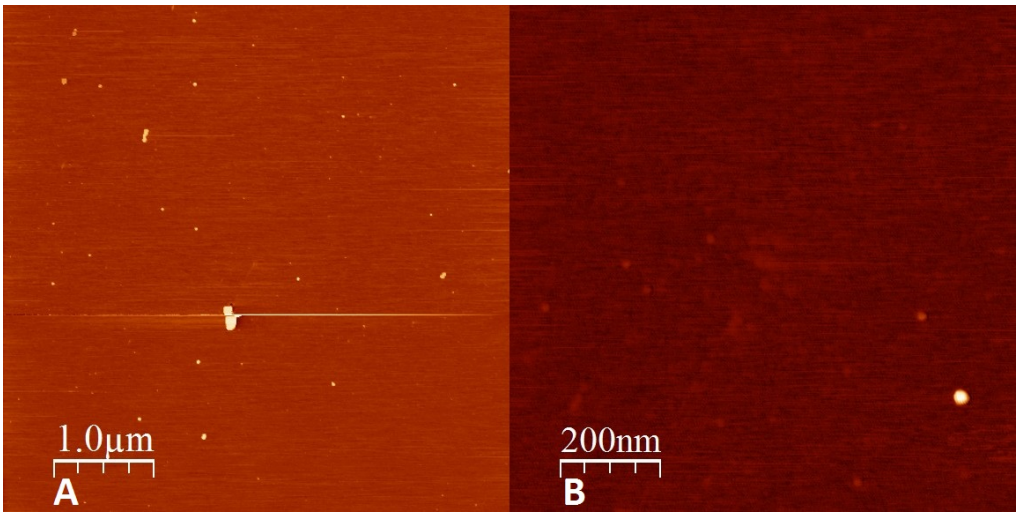

Figure 3.3: Two AFM scans of a mica surface with immobilized amidated KA_5 dissolved in H_2O. A is a 5x5 μm image of the AFM scan, B is a zoom in to 1x1 μm.

Figure 3.3A is an 5x5 mum AFM scan of a mica surface where HPLC purified amidated KA_5

has been immobilized. The scan area has a couple of round structures that stand out from the mica surface. Two round structures are close to the center of the scanned area while some smaller round structures are on the entire scan area. The large structures are around 40 nm in height and have widths of around 100 nm. The smaller structures have heights of around 5 nm and diameters of 20-50 nm. Figure 3.3B is a zoom in to 1x1 μm scan area, where one of the round structures are visible. This is around 5 nm in height and has a diameter of around 25 nm.

After the AFM run of the amidated KA_5, Figure 3.3, the pH was found to be around 10 and was therefore adjusted to neutral and the solution were exposed to ultrasound for around five minutes, immobilized on mica for 20 to 30 minutes, and scanned with AFM, Figure 3.4.

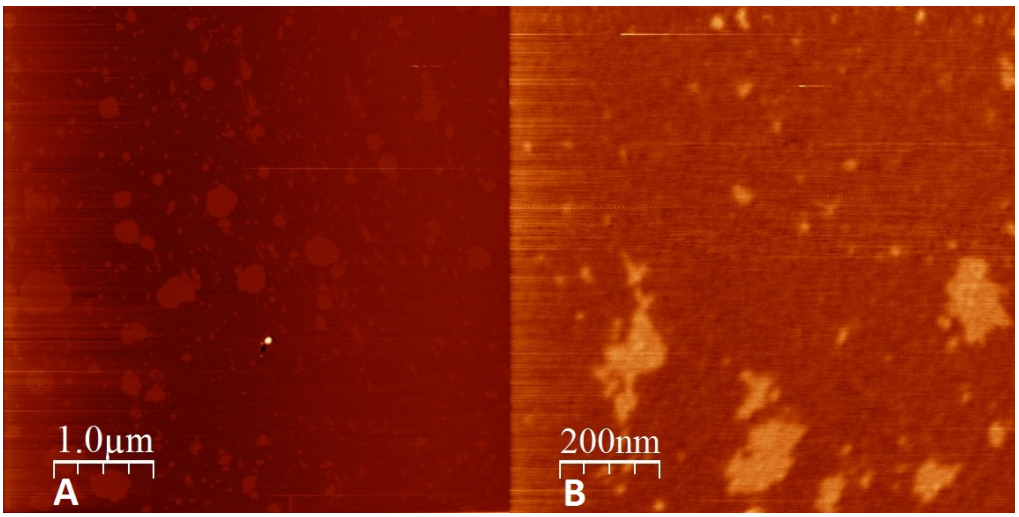

Figure 3.4: Two AFM scans of a mica surface with immobilized amidated KA_5 dissolved in H_2O and adjusted to neutral pH. A is a 5x5 μm image of the AFM scan, B is a zoom in to 1x1 μm.

A round structure is present in the center of the 5x5 μm scan area, Figure 3.4A. This has a height around 15 nm and diameter of around 100 nm. A layer is also present on the surface, this has height of around 1 nm and has various shapes and sizes.

No further experiments was done with the amidated KA_5 due to lack of material. Amidated KA_5 was the peptide that was used for tuning experiments, e.g. the HPLC programs.

3.2 Non-amidated KA_5

3.2.1 HPLC Purification

Non-amidated KA_5 was purified through HPLC before any self-assembly was attempted. The peptide was run through the small column using the gradient illustrated by Figure 2.1A, resulting in the spectrum on Figure 3.1.

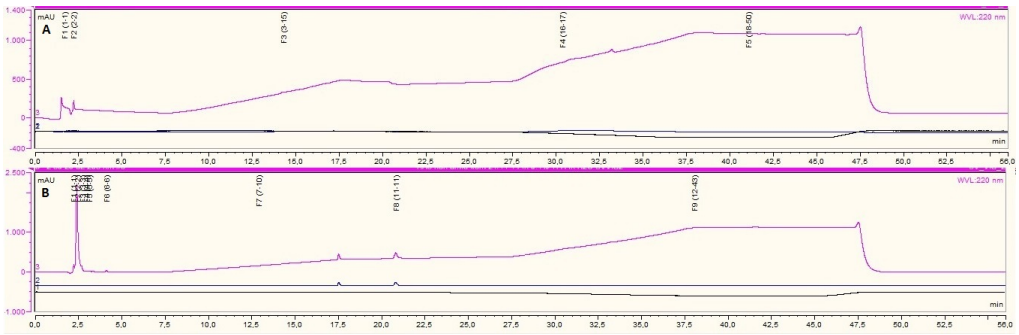

Figure 3.5: Spectres from two runs of HPLC where the small column and a 20 μL chamber is used. The dark blue line is the absorbance in mAU at 280 nm, the purple line is the absorbance in mAU at 220 nm, and the black line is the pump pressure in bar. Maximums were recognized based on the absorbance at 220 nm. The numbers above the maximums represents the vial in which a maximum was collected. A is the spectrum of a HPLC run with pure 0.1% TFA dissolved in H_2O, control and B is the spectrum of a run where the synthesized non-amidated KA_5 is dissolved in the control solution, 0.1% TFA dissolved in H_2O.

More or less everything was recognized as signals and were collected. The program was changed and the requirements for signals were increased to make the HPLC recognize less as signals. The column was changed to the large column and the chamber was changed to the 2 mL chamber, Figure 3.6.

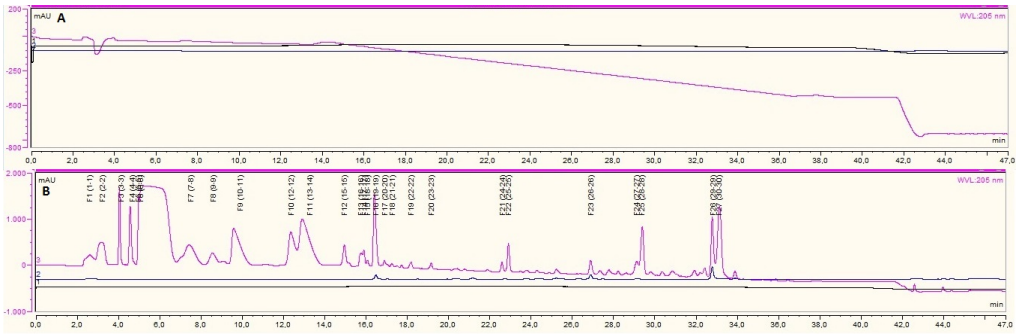

Figure 3.6: Spectres from two runs of HPLC where the large column and a 2 mL chamber is used. The dark blue line is the absorbance in mAU at 280 nm, the purple line is the absorbance in mAU at 220 nm, and the black line is the pump pressure in bar. maximums were recognized based on the absorbance at 220 nm. The numbers above the maximums represents the vial in which a maximum was collected. A is the spectrum of a HPLC run with pure 0.1% TFA dissolved in H_2O, control and B is the spectrum of a run where the synthesized non-amidated KA_5 is dissolved in the control solution, 0.1% TFA dissolved in H_2O.

30 maximums were collected from the HPLC run with non-amidated KA_5 in the large column with the 2 mL chamber. To identify which vial contained the peptide the vials were freeze-dried and it was found that vial six contained peptide and was used for experiments.

3.2.2 Self-assembly

Self-assembly was attempted with the non-amidated KA_5 after the HPLC purification, this yielded two AFM scans, Figure 3.7.

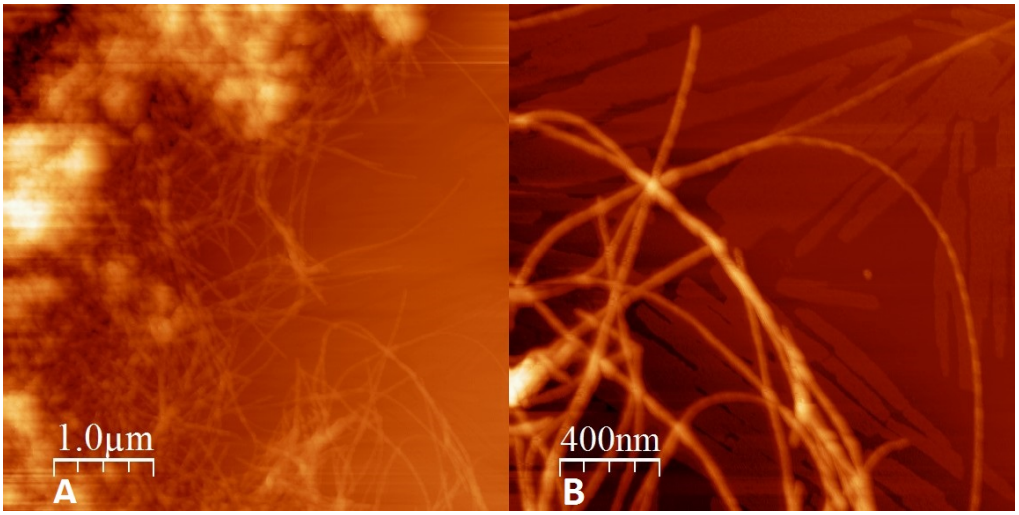

Figure 3.7: Two AFM scans of a mica surface with immobilized non-amidated KA_5 dissolved in H_2O. A is a 5x5 μm scan and B is a 2x2 μm scan.

The 5x5 μm AFM scan, Figure 3.7A, has some large aggregates with heights around 100 nm. Rod-shaped structures are also present, these have heights of around 5 nm and widths of around 30 nm. The 2x2 μm AFM scan, Figure 3.7B, is a zoom in onto some of the rod-shaped structures, but also shows some flat rod-shaped structure with heights of 1-2 nm and widths of around 50 nm. These seem to be spread evenly to the entire surface.

It was attempted to dissolve the aggregates by exposing the solution to ultrasound for around 30 minutes. After these 30 minutes another sample was immobilized on mica and scanned with AFM, Figure 3.8.

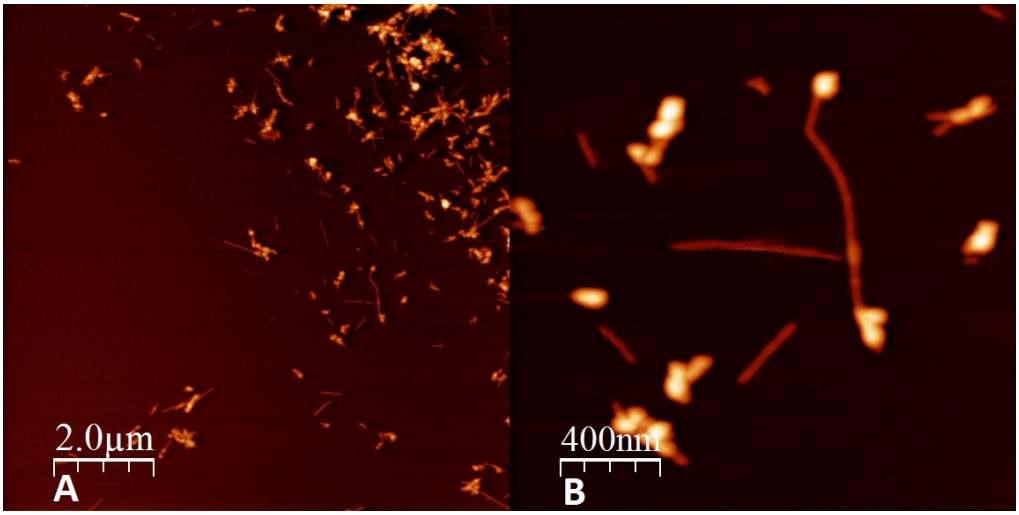

Figure 3.8: Two AFM scans of non-amidated KA_5 exposed to ultrasound for 30 minutes. A is a 10x10 μm scan and B is a 2x2 μm scan.

The large aggregate was partly dissolved. There are still some aggregates present on the 10x10 μm scan, Figure 3.8A, these are around around 30 nm high. Rod-shaped structures are also present, these have heights of 3-5 nm and widths of around 25 nm. There is also a round structure present with heights around 15 nm and diameters of around 100 nm. The rod-shaped and the round structure are clearly visible on the 2x2 μm scan, Figure 3.8B.

3.2.2.1 HCl Washed

After the HCl wash the remaining peptide was dissolved in H_2O. This was split into three and these solutions was pH adjusted to acidic, neutral and basic. Each of these solutions were exposed to ultrasound for five minutes and immobilized on mica and scanned with AFM. The acidic, Figure 3.9A, the neutral, Figure 3.9B, and the basic, Figure 3.9C, all had similar structures, round structures with heights varying between 5 nm and 100 nm and diameters from around 30 nm to around 200 nm.

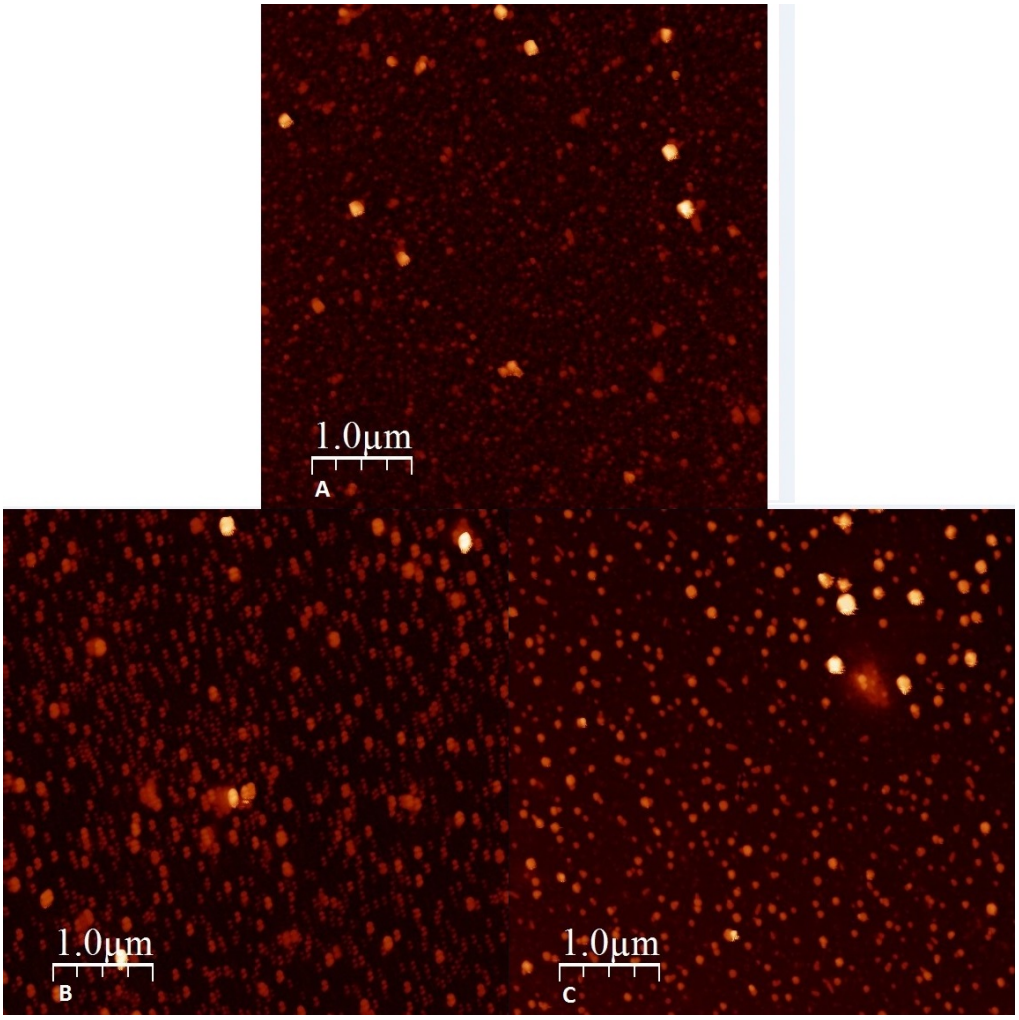

Figure 3.9: Three AFM scans of non-amidated KA_5 after the HPLC wash. All scans are after one hour of self-assembly and have scan areas of 5x5 μm, A is acidic, B is neutral, and C is basic.

After 24 hours another sample was taken from each of the solutions. Structures from the acidic, Figure 3.10A, and neutral, Figure 3.10B, sample are similar. These are round or cubic structures with heights up to 100 nm and widths up to 300 nm. Both have a rough surface with varying height around 2 nm.
The sample from the basic solution, 3.10C, has a rough layer with heights around 2 nm. Rod-shaped structures are also present with heights around 70 nm, diameter around 200 nm, and length around 1 μm. The rods are in the center of some of the round areas on the surface. In these areas the surface is more rough than the rest, the height variation in these areas are up to 20 nm.

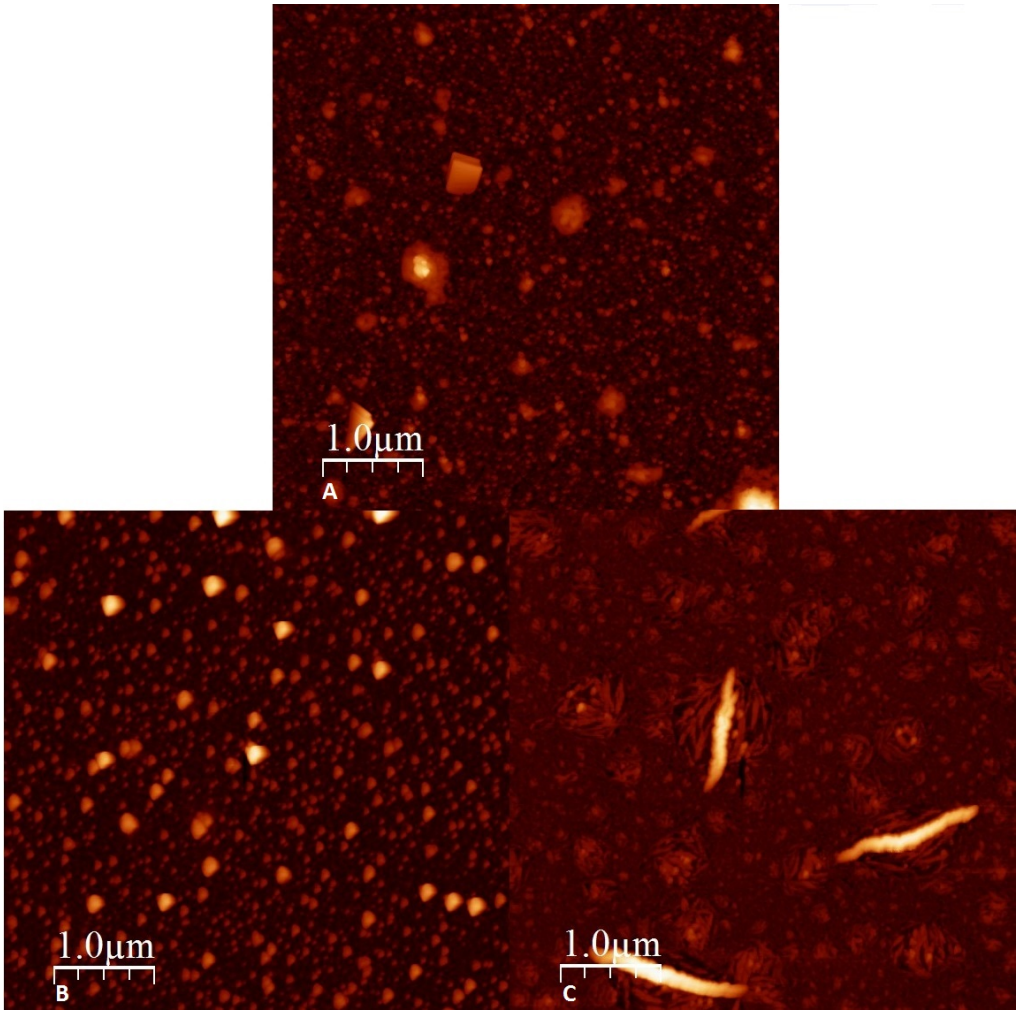

Figure 3.10: Three AFM scans of non-amidated KA_5 after the HPLC wash. All scans are after 24 hours of self-assembly and have scan areas of 5x5 μm, A is acidic, B is neutral, and C is basic.

3.2.3 Thioflavin-T

Two detectors were used during the experiment with thioflavin-T. With thioflavin-T dissolved in H_2O without peptide the emission of the first detector, 3.11A, was fluctuating below 5 μM, after which the increase was steady until the max emission at 20 μM. The second detector, Figure 3.11B, measured a steady increase from 0.5 μM until the max emission at 20 μM.

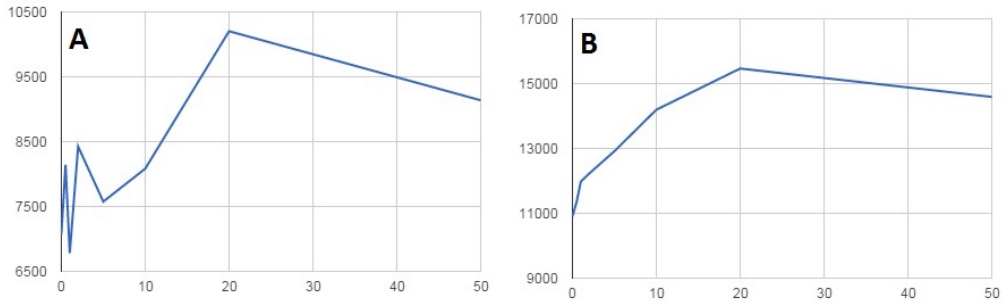

Figure 3.11: Illustration of the emission measured of thioflavin-T dissolved in H_2O. The first axis is the concentration of thioflavin-T and the second axis is the emission. A is detector one and B is detector two.

A Sample from the solution with 50 μM was immobilized on mica and imaged with AFM to compare the structures formed by thioflavin-T alone to structures formed by thioflavin-T and peptide.

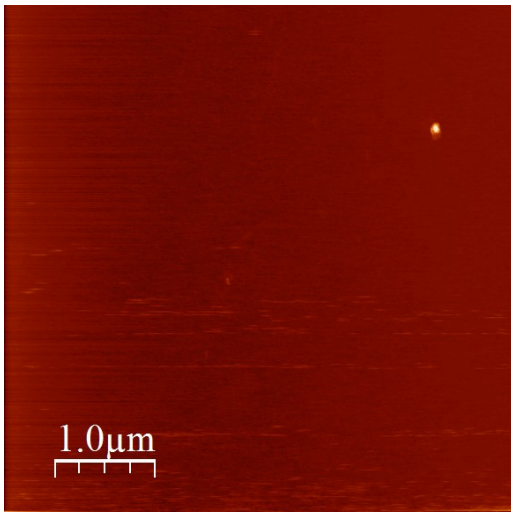

Figure 3.12: An AFM scan of a mica surface where it was attempted to immobilize thioflavin-T.

The surface of mica with immobilized thioflavin-T, Figure 3.12, is flat and the largest height variation is around 0.3 nm.

After a few months of working with KA_4 and KA_6, the solutions of non-amidated KA_5 were used for fluorescent experiments with thioflavin-T. It was found that the emission increased until a max value at 10 μM, for the first detector, and 20 μM for the second detector. After this max value the emission was stable until 50 μM, the highest concentration measured. The emission of thioflavin-T in the neutral KA_5 solution is illustrated by Figure 3.13, where

Figure 3.13A is detector one and Figure 3.13B is detector two.

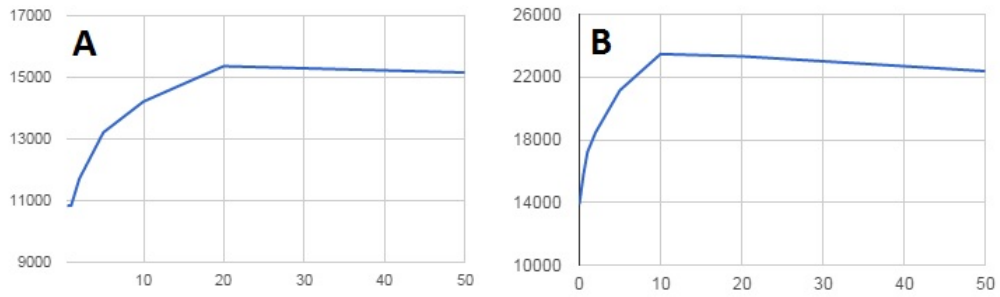

Figure 3.13: Illustration of the emission measured of thioflavin-T and KA_5 dissolved in H_2O. The first axis is the concentration of thioflavin-T and the second axis is the emission. A is detector one and B is detector two.

The experiment was done with all three solutions, but due to a low amount of solution only the neutral solution yielded a measurement that was not solely noise. Samples from all three solutions, now containing 50 mM thioflavin-T, were immobilized on mica and scanned with AFM. Samples were taken after 1 and 72 hours of self-assembly, however the acidic and the neutral solutions had similar structures after 1 hour and 72 hours. All samples containing KA_5 and thioflavin-T were rinsed with H_2O after the peptide was immobilized and blow-dried.

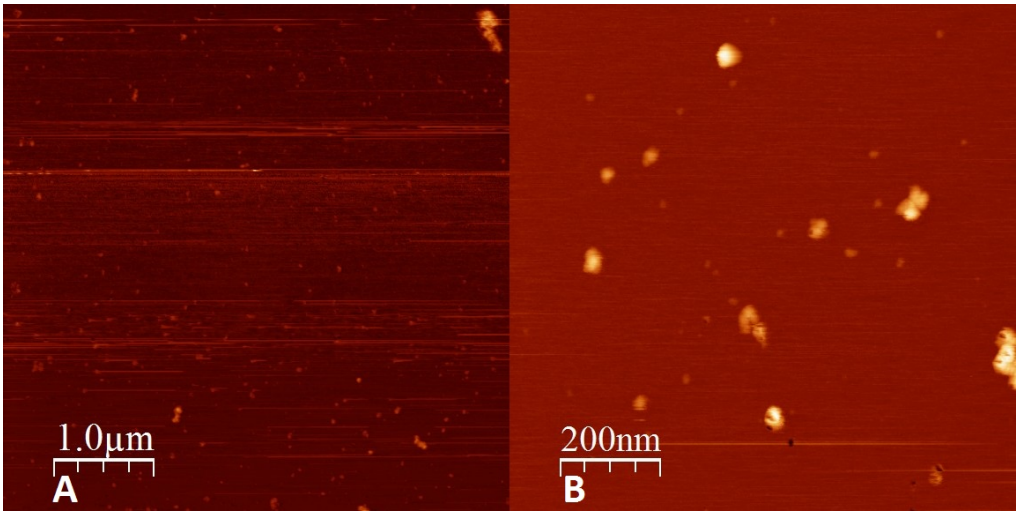

Figure 3.14: Two AFM scans of a mica sample with immobilized KA_5 containting 50 mM thioflavin-T in acidic solution after one hour of self-assembly. A is a scan area of 5x5 μm and B is a scan area 1x1 μm.

The 5x5 μm AFM scan of the mica surface where KA_5 and thioflavin-T in acidic solution has been immobilized, Figure 3.14A, has round structures. The 1x1 μm AFM scan, Figure 3.14B, is a zoom in of some of these structures. The height of these structures is around 10 nm and the

diameter is between 30 and 50 nm. Another sample was taken after 72 hours of self-assembly and the scan was similar to the scan after 1 hour.

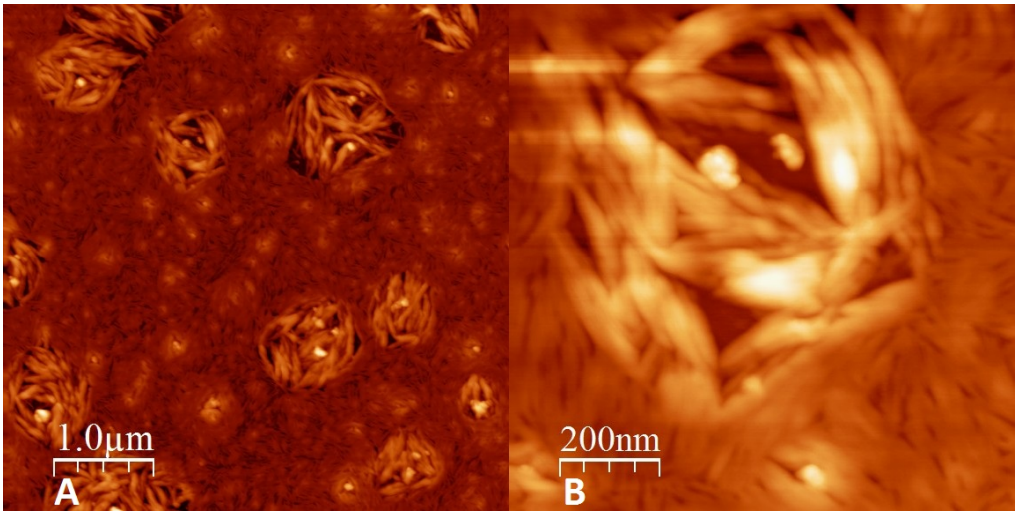

Figure 3.15: Two AFM scans of a mica sample with immobilized KA_5 containting 50 mM thioflavin-T in neutral solution after one hour of self-assembly. A is a scan area of 5x5 μm and B is a scan area 1x1 μm.

After one hour of self-assembly a sample from the neutral solution was immobilized on mica, Figure 3.15. Two scans were made, one with a scan area of 5x5 μm, Figure 3.15A, and one with a scan area of 1x1 μm, Figure 3.15B. The mica surface has a high concentration of a rod-shaped structure that is evenly spread to the scan area. These rods have heights of around 4 nm and widths of around 40 nm, however the widths are varying. Round structures are also present, these have heights of around 15 nm and varying diameters around 50 nm. Aggregates are also present with heights up to around 40 nm. Another sample was taken after 72 hours of self-assembly and the scan was similar to the scan after 1 hour.

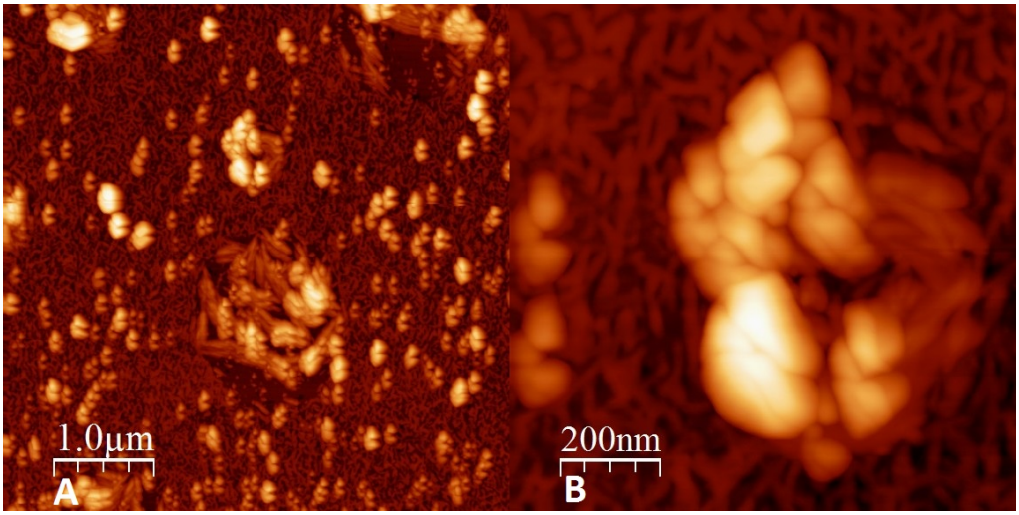

Figure 3.16: Two AFM scans of a mica sample with immobilized KA_5 containting 50 mM thioflavin-T in basic solution after one hour of self-assembly. A is a scan area of 5x5 μm and B is a scan area 1x1 μm.

After one hour of self-assembly a sample from the basic solution was immobilized on mica, Figure 3.16. Two scans were made, one with a scan area of 5x5 μm, Figure 3.16A, and one with a scan area of 1x1 μm, Figure 3.16B. Round structures are present but the structures does not appear as single structures, but in pairs or groups. The round structures have heights of around 20 nm and diameters between 50 nm and 100 nm. Rod-shaped structures are present these are flat on the surface below the round structures. They have heights up to 6 nm and diameters between 20 nm and 50 nm. Aggregates are also present on the scanned surface, these have heights up to 80 nm.

After 72 hours of self-assembly a sample from the basic solution was immobilized on mica, Figure 3.17. Two scans were made, one with a scan area of 5x5 μm, Figure 3.17A, and one with a scan area of 1x1 μm, Figure 3.17B. Round structures are present on the surface, these have heights around 4 nm and diameters around 50 nm. Aggregates are also present with heights up to 100 nm.

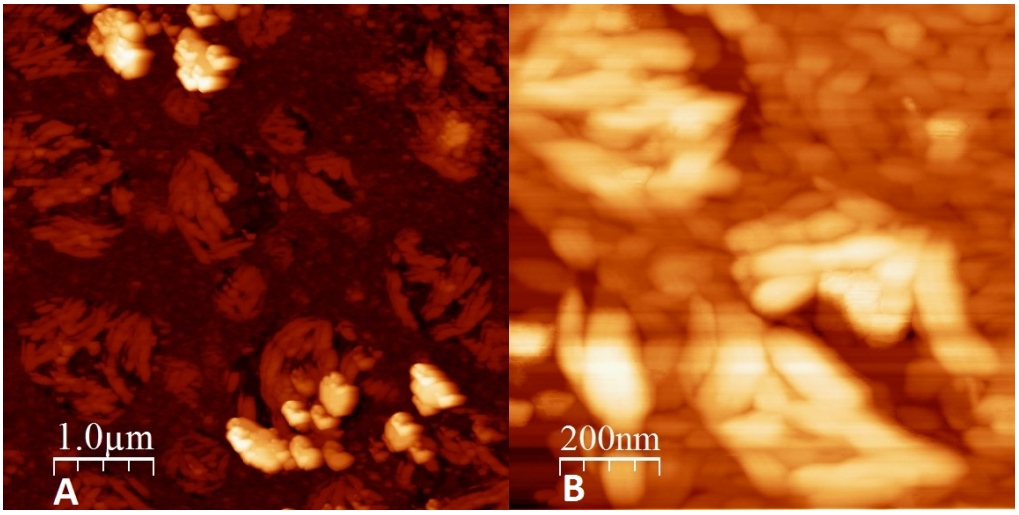

Figure 3.17: Two AFM scans of a mica sample with immobilized KA_5 containting 50 mM thioflavin-T in basic solution after 72 hours of self-assembly. A is a scan area of 5x5 μm and B is a scan area 1x1 μm.

3.2.4 In Silico

An in silico experiment was done with 50 non-amidated KA_5 in a 5x5x5 nm box. The result of the experiment was a rod-shaped structure. Figure 3.18 illustrates the structure from four directions. The rod is the full length of the box, 5 nm, while the width is around 3 nm.

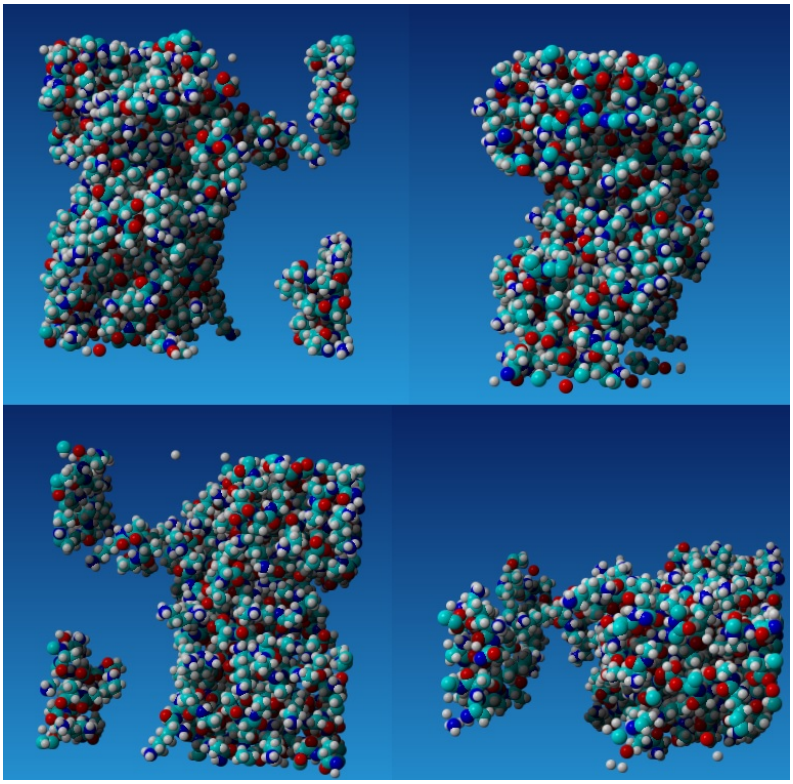

Figure 3.18: The result from the in silico experiment with 50 KA_5 in a 5x5x5 nm box visualized from four directions.

3.3 Non-amidated KA_6

3.3.1 HPLC Purification

Before any self-assembly was attempted with KA_6, the peptide was purified through HPLC. The peptide was run through the small column using the gradient illustrated by Figure 2.1A, resulting in the spectrum on Figure 3.19B along with a control with only 0.1% TFA dissolved in water, Figure 3.19A.

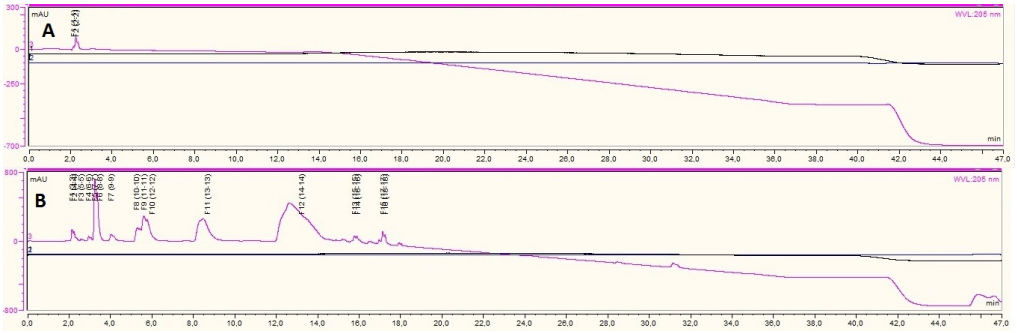

Figure 3.19: Spectres from two runs of HPLC where the small column and 20 μL chamber is used. The dark blue line is the absorbance in mAU at 280 nm, the purple line is the absorbance in mAU at 205 nm, and the black line is the pump pressure in bar. Maximums were recognized based on the absorbance at 205 nm. The numbers above the maximums represents the vial in which a maximum was collected. A is the spectrum of a HPLC run with pure 0.1% TFA dissolved in H_2O, control and B is the spectrum of a run where the synthesized KA_6 is dissolved in the control solution, 0.1% TFA dissolved in H_2O.

16 signals were collected, however since the chamber only contained 20 μL sample and only a small amount of peptide was dissolved it was not possible to determine which signal was caused by the peptide. The program was changed to delay the signal from the peptide. The gradient used is illustrated by 2.1B.
The large column and the 2 mL chamber was used to purify the rest of the peptide and the spectrum from this run and a control can be seen on Figure 3.20.

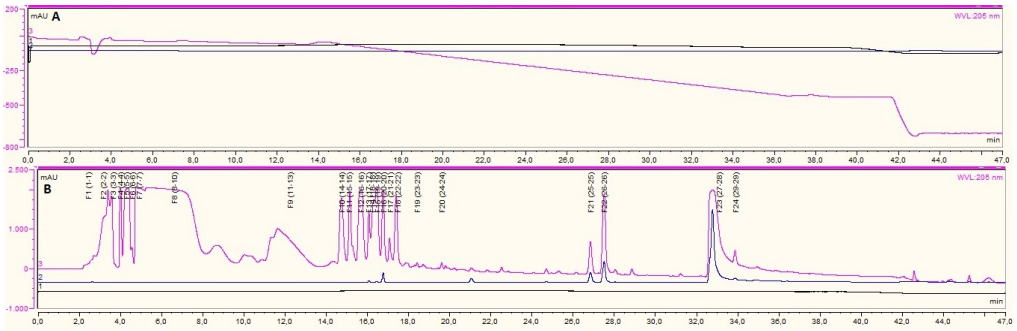

Figure 3.20: Spectres from two runs of HPLC where the large column and 2 mL chamber is used. The dark blue line is the absorbance in mAU at 280 nm, the purple line is the absorbance in mAU at 205 nm, and the black line is the pump pressure in bar. Maximums were recognized based on the absorbance at 205 nm. The numbers above the maximums represents the vial in which a maximum was collected. A is the spectrum of a HPLC run with pure 0.1% TFA dissolved in H_2O, control and B is the spectrum of a run where the synthesized KA_6 is dissolved in the control solution, 0.1% TFA dissolved in H_2O.

24 signals were collected from the HPLC run of KA_6 through the large column, Figure 3.20B. To determine which signal was caused by the peptide, each flow-through were freeze-dryed. Vial 8 contained the most peptide and was used for further experiments.

3.3.2 Self-assembly

3.3.2.1 HPLC Purified

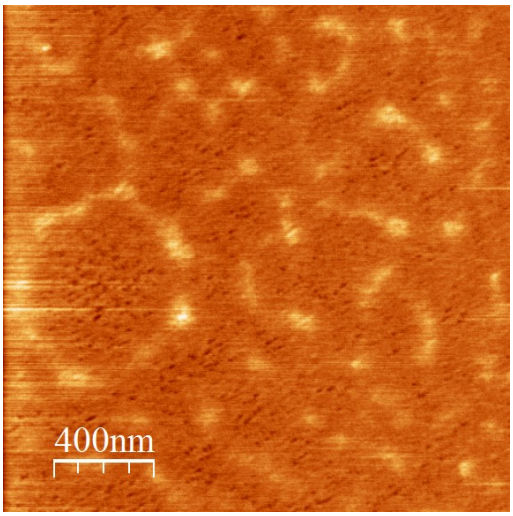

Figure 3.21: An AFM scan of a mica surface where the synthesized KA_6, in an acidic solution, was attempted to immobilize after one hour of self-assembly.

Some structure is present on the mica surface where the HPLC purified KA_6 in an acidic solution has been immobilized, Figure 3.21. These structures are neither wires, tubes, micelles or vesicles. The structures are roughly 1 nm in height and spread on the entire surface.

The structures present on the mica surface where the HPLC purified KA_6 in a neutral solution has been immobilized, Figure 3.22, are flat rod-shaped or shaped like flakes with heights of around 10 nm. Figure 3.22A also have both individual flake-like structures, but also clusters or aggregates of these flakes where the highest clusters are around 40 nm. Figure 3.22B is a zoom in of one of these aggregates, this one having a height of around 25 nm. The width of the individual flakes varies from around 100 nm to around 400 nm.

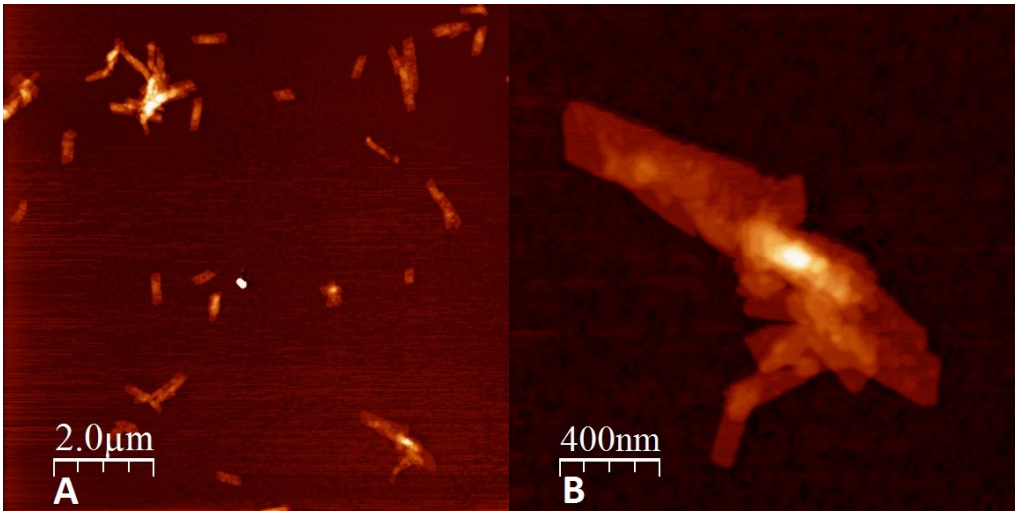

Figure 3.22: AFM scans of a mica surface where the synthesized KA_6, in a neutral solution, were immobilized after one hour of self-assembly. A is a scan area of 10x10 μm and B is 2x2 μm and is a zoom in of one of the structures.

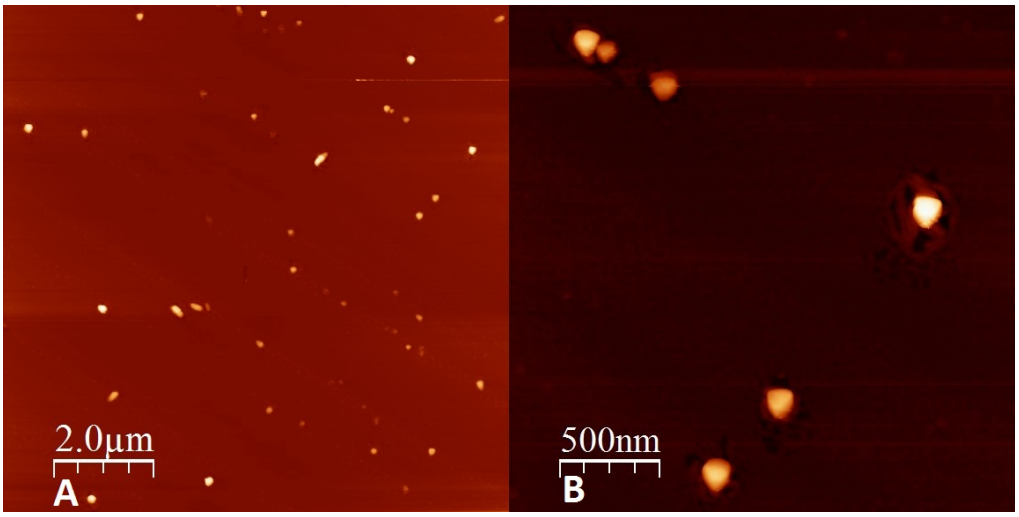

Figure 3.23: AFM scans of a mica surface where the synthesized KA_6, in a basic solution, was immobilized after one hour of self-assembly. A is an image of a 10x10 μm scan area while B has a 2.5x2.5 μm scan area.

The sample of KA_6 with basic pH was immobilized on mica and scanned. An area of 10x10 μm, Figure 3.23A, was scanned. Round structures were seen on the scan with heights up to around 70 nm, and widths of around 100 nm. A zoom in was made of some of the structures, Figure 3.23B. This zoom in shows the structures are not spherical but are more cubic shaped and has edges sharper than a sphere would.

The sharply edged structures seen on 3.23B indicates that salt is present and that the structures seen are salt crystals and not structures self-assembled by peptide. Therefore the peptide was washed with HCl which could exchange an anion bound to the positive N-terminus of the peptide with a chloride ion.

3.3.2.2 HCl Washed

The HCl washed peptide was used to make three solutions, one acidic, one neutral, and one basic. The solutions were left to self-assembly for around one hour before samples were taken.

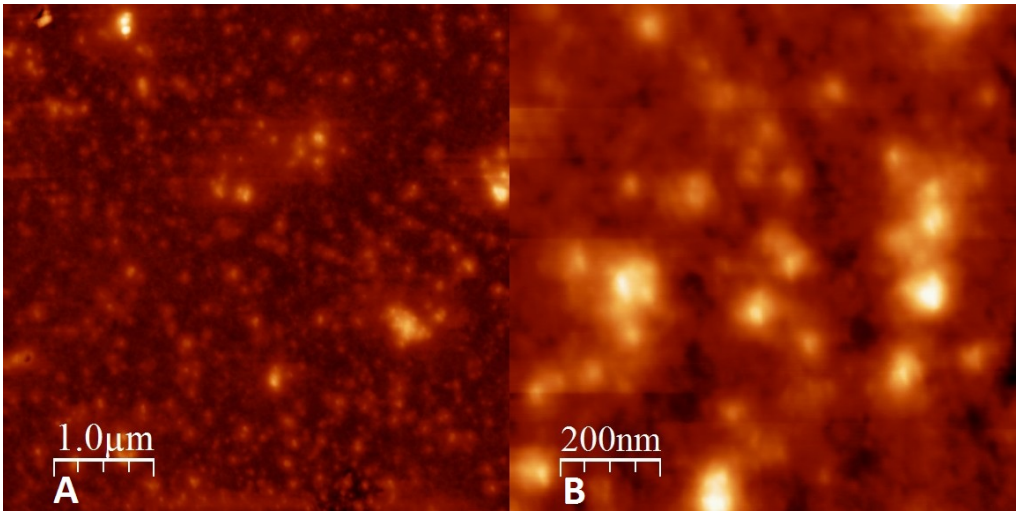

Figure 3.24: AFM scans of a mica surface where the HCl washed KA_6, in an acidic solution, was immobilized after one hour of self-assembly. A is an image of a 5x5 μm scan area while B has a 1x1 μm scan area.

The acidic sample of the HCl washed KA_6 was immobilized on mica and scanned with AFM. An area of 5x5 μm was scanned, Figure 3.24A, and round structures were present. A zoom in to 1x1 μm was made, Figure 3.24B. The round structures has heights of up to 50 nm, however most have heights of around 15 nm. The widths of the structures are between 50 and 100 nm.

A 5x5 μm scan of the mica surface where the HPLC purified and HCl washed KA_6 in a neutral solution has been immobilized, Figure 3.25A, shows a rough surface with some large structures standing out. These structures have heights of up to 150 nm and widths of up to 500 nm. A zoom in to 1x1 μm, Figure 3.25B, was made and some smaller and round structures are clearly visible. These have heights of around 15 nm and diameters between 20 and 40 nm.

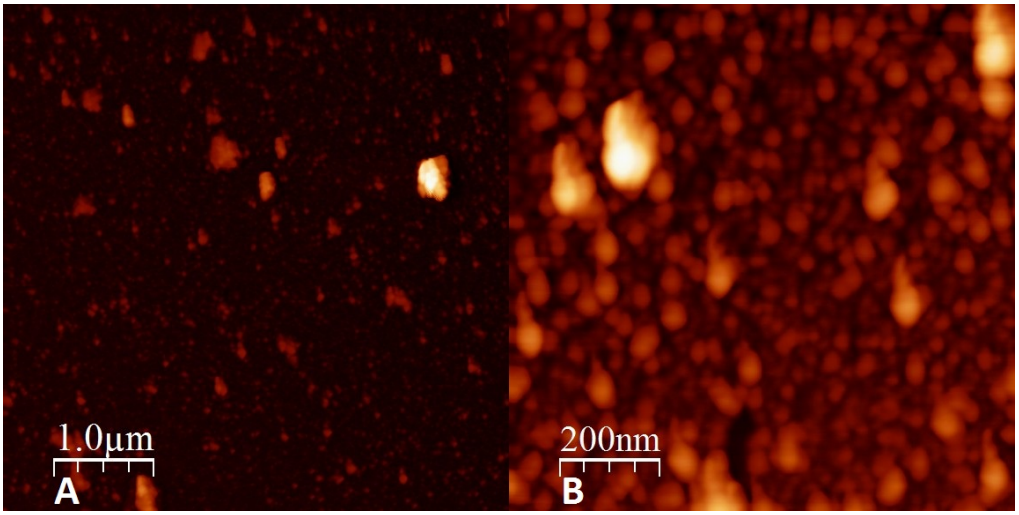

Figure 3.25: AFM scans of a mica surface where the HCl washed KA_6, in a neutral solution, was immobilized after one hour of self-assembly. A is an image of a 5x5 μm scan area while B has a scan area of 1x1 μm.

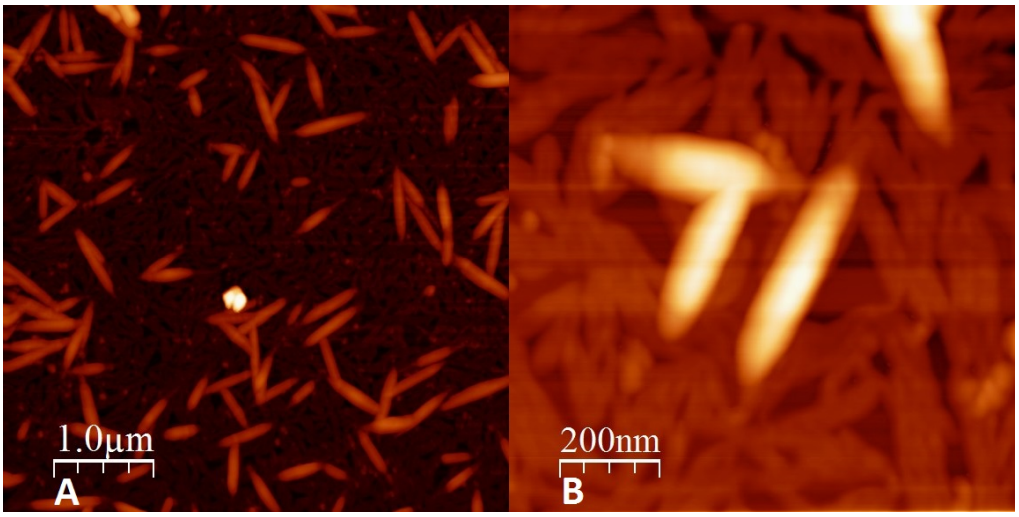

Figure 3.26: AFM scans of a mica surface where the HCl washed KA_6, in a basic solution, was immobilized after one hour of self-assembly. A is an image of a 5x5 μm scan area while B has a scan area of 1x1 μm.

The basic solution of KA_6 was immobilized on mica after one hour of self-assembly and an area of 5x5 μm was scanned with AFM, Figure 3.26A. Rod-shaped structures are visible on this scan with heights around 20 nm and diameters of around 50-100 nm. A zoom in was done to 1x1 μm, Figure 3.26B. On the zoom in another structure is visible. This structure is also rod-shaped but only has heights of around 5 nm and diameters of around 40 nm. The low structure is evenly spread to the entire surface and no individual of these rods are seen.

Each of the three solutions were immobilized on mica and scanned with AFM after 24 hours of self-assembly.

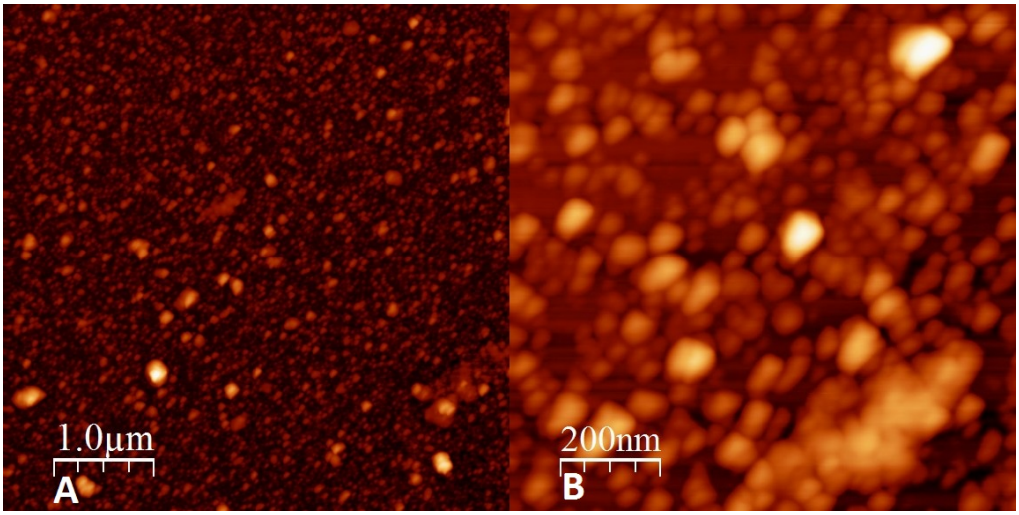

Figure 3.27: AFM scans of a mica surface where the HCl washed KA_6, in an acidic solution, was immobilized after 24 hours of self-assembly. A is an image of a 5x5 μm scan area while B has a 1x1 μm scan area.

The acidic solution of KA_6 was immobilized on mica after 24 hours of self-assembly and scanned with AFM. The first scan was a 5x5 μm, Figure 3.27A. This scan has some round structures with diameters between 10 and 50 nm and heights of 5 to 25 nm. A zoom in to 1x1 μm, Figure 3.27B, was done where the smallest of the structures are visible, where it can also be seen that the structures are not perfectly round.

24 hours after the neutral solution containing KA_6 was left to self-assembly another sample was immobilized on mica and investigated with AFM. Round structures are visible on the 5x5 μm scan, Figure 3.28A. Most have diameters of around 50 nm and heights of 10-15 nm. Larger structures are also present, these have diameters up to 200 nm and heights up to 100 nm. A zoom in was made of some of the structures to 1x1 μm, Figure 3.28B. On the zoom in the small round structures are visible together with a larger cluster. The cluster are around 800x400 nm and have varying height up to 100 nm.

The structures formed after 24 hours of self-assembly of KA_6, Figure 3.28, are similar to the structures formed after one hour of self-assembly.

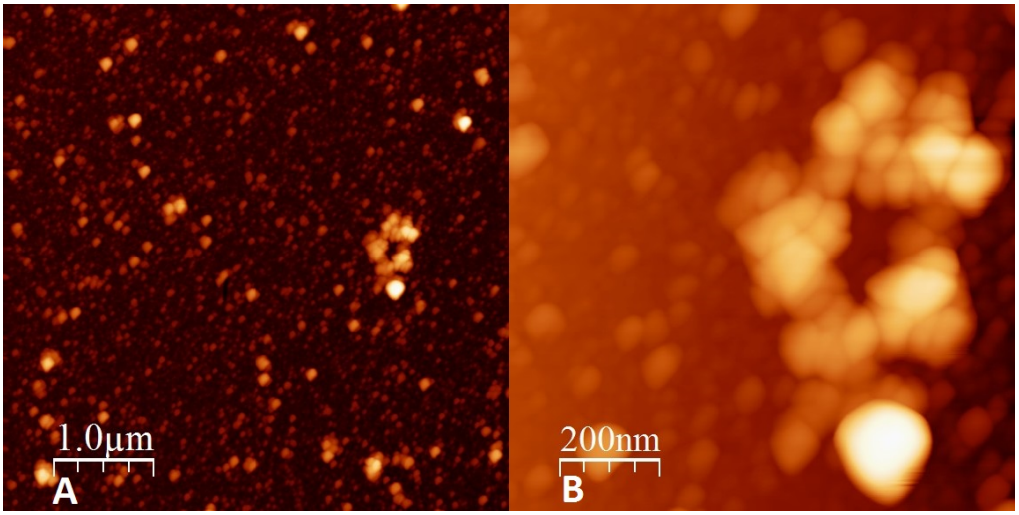

Figure 3.28: AFM scans of a mica surface where the HCl washed KA_6, in a neutral solution, was immobilized after 24 hours of self-assembly. A is an image of a 5x5 μm scan area while B has a scan area of 1x1 μm.

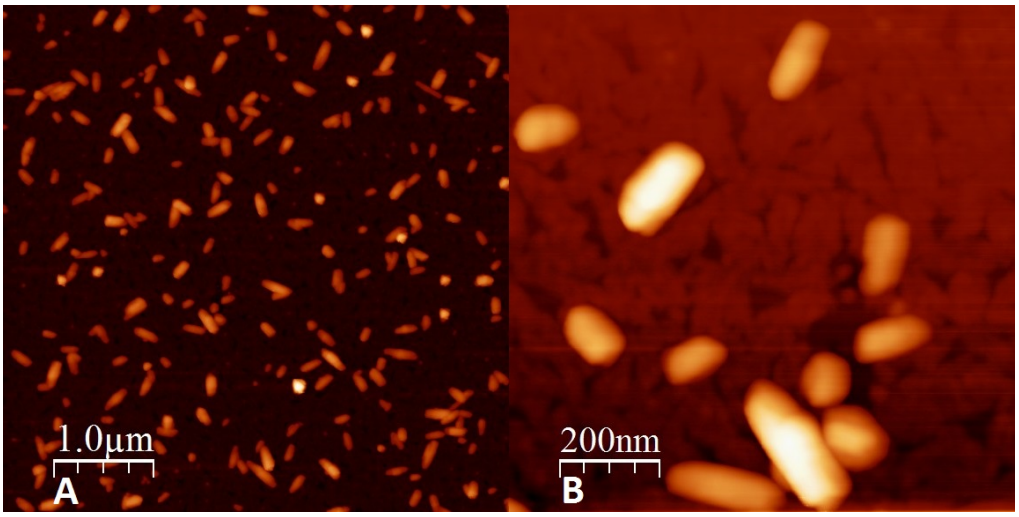

Figure 3.29: AFM scans of a mica surface where the HCl washed KA_6, in a basic solution, was immobilized after 24 hours of self-assembly. A is an image of a 5x5 μm scan area while B has a scan area of 1x1 μm.

The AFM scan of the mica surface where the basic solution of KA_6 were immobilized has some rod-shaped structures. A large amount of the rod-shaped structures are visible on the 5x5 μm scan, Figure 3.29A, while a few are clearly visible on the 1x1 μm scan, Figure 3.29. The rod-shaped structures have heights of 20-50 nm, diameters of 50-100 nm, and lengths of around 200 nm. On the zoom in, Figure 3.29B, another structure is also visible. There is a high concentration so no individual structure can be seen and therefore the length of the structure cannot

be measured. The structures seems to be rod-shaped with heights of 2-3 nm and diameters similar to the other structures.

3.3.2.3 New Solution

A new solution of KA_6 in H_2O was made with the remaining peptide. The concentration was calculated to ~7 mM via absorbance measurements at 205 nm. Due to the small amount of solution only neutral pH was used for the remaining experiments. Experiments with thioflavin-T was planned to determine if structures are present in the solution or if they are formed on the surface of mica before an AFM scan.

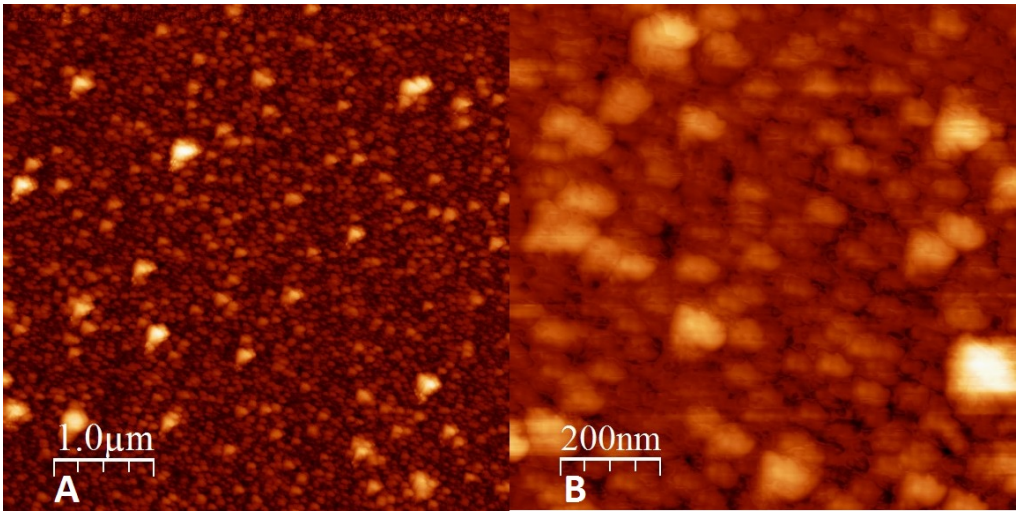

Figure 3.30: AFM scans of a mica surface where the HCl washed KA_6, in a neutral solution, was immobilized after one hour of self-assembly. A is an image of a 5x5 μm scan area while B has a scan area of 1x1 μm.

A sample was prepared for AFM on mica. The 5x5 μm scan, Figure 3.30, shows some round structures spread to the entire scan area. Most of the structures have heights of around 15 nm, however some have heights of up to 50 nm. The diameter of these structures are around 50-100 nm.
After a couple of days when experiments with thioflavin-T was supposed to be made, the solution with KA_6 was unclear and had solid residues. Experiments with KA_6 and thioflavin-T was abandoned due to the solid residues and the solution had emission at a wide range of wavelenghts around the emission of thioflavin-T.

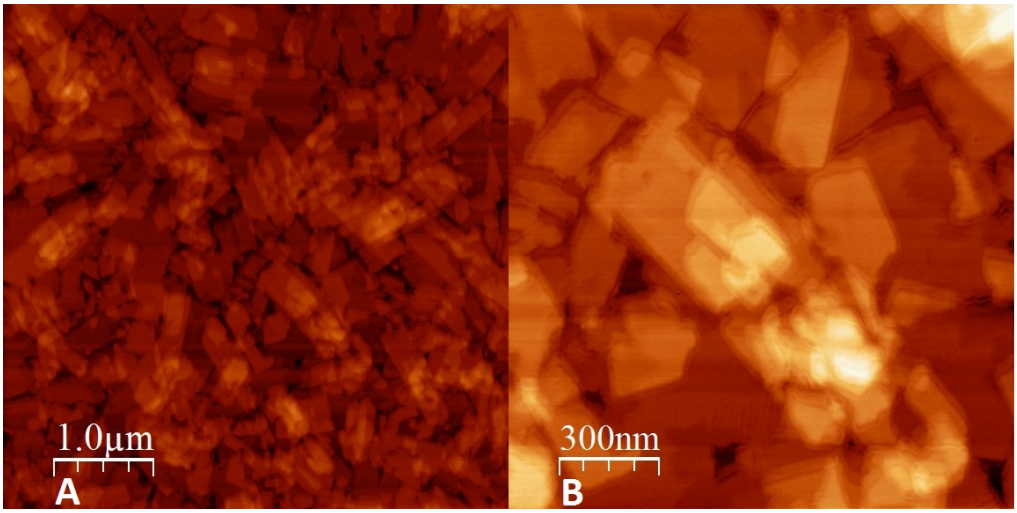

Figure 3.31: AFM scans of a mica surface where the HCl washed KA_6, in a neutral solution, was immobilized after a couple of days of self-assembly. A is an image of a 5x5 μm scan area while B has a scan area of 1.5x1.5 μm.

A sample was immobilized on mica and imaged with AFM, this resulted in Figure 3.31A. The structures present in the scanned area are flat. A zoom in from 5x5 μm to 1.5x1.5 μm, Figure 3.31B, was made to determine the dimensions of the structures. The structures were found to have heights of around 20 nm and widths of 100-400 nm.

3.3.3 In Silico

An in silico experiment was done with 50 KA_6 in a 5x5x5 nm box. The result of the experiment was a layer with height of around 2 nm. Figure 3.32 illustrates the structure from four directions. The layer is the full length and width of the box, however areas exists where the layer is not completely solid.

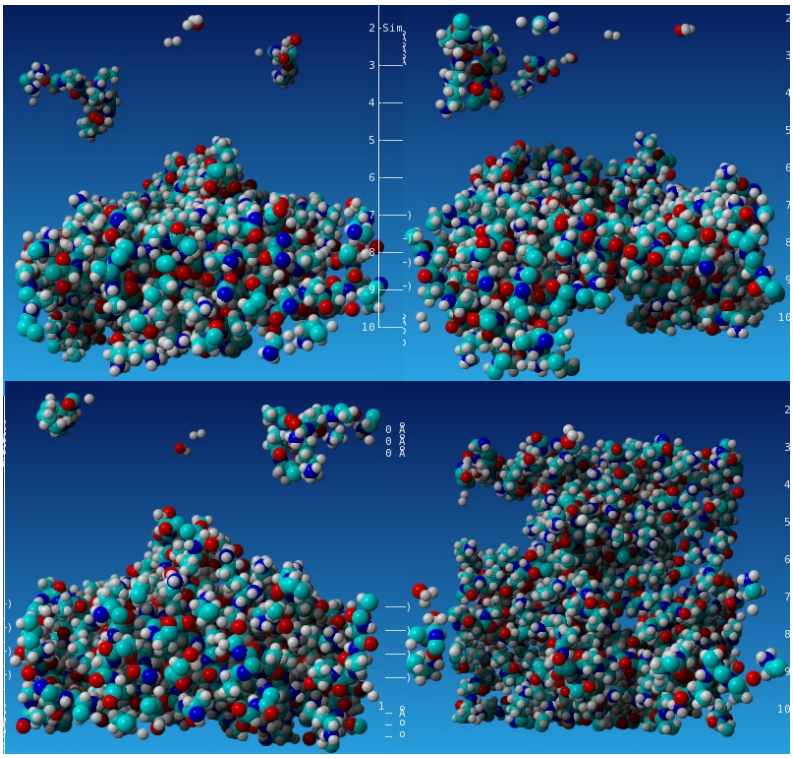

Figure 3.32: The result from the in silico experiment with 50 KA_6 in a 5x5x5 nm box visualized from four directions.

3.4 Non-amidated KA_4

3.4.1 HPLC Purification

Before attempting any self-assembly on the synthesized KA_4, the peptide was purified through HPLC to remove by-products leading to a KA_4 of higher purity. The program used for the purification is illustrated by Figure 2.1A. No HPLC run were done with the small column and the 20 μL chamber, as it was not deemed necessary. The purification of KA_4 was done through only the large column and using the 2 mL chamber, the spectres from this purification is shown on Figure 3.33.

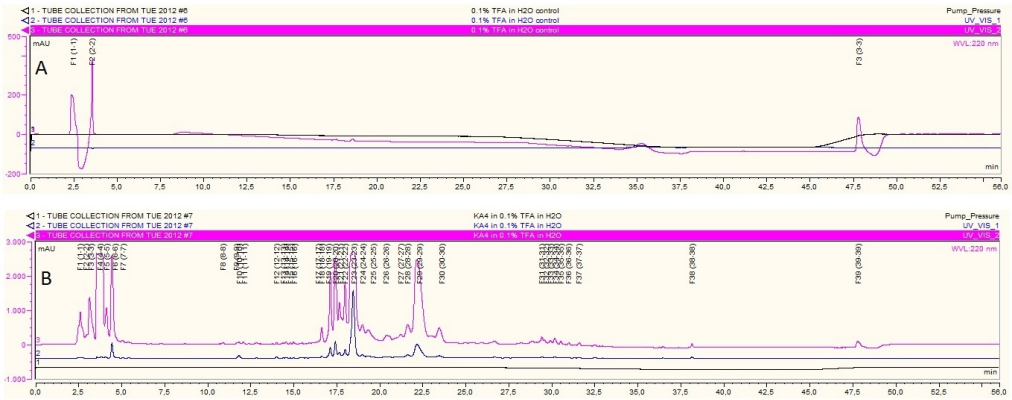

Figure 3.33: Spectres from two runs of HPLC where the large column and a 2 mL chamber is used. The dark blue line is the absorbance in mAU at 280 nm, the purple line is the absorbance in mAU at 220 nm, and the black line is the pump pressure in bar. Maximums were recognized based on the absorbance at 220 nm. The numbers above the maximums represents the vial in which a maximum was collected. A is the spectrum of a HPLC run with pure 0.1% TFA dissolved in H_2O, control and B is the spectrum of a run where the synthesized KA_4 is dissolved in the control solution, 0.1% TFA dissolved in H_2O.

There are 39 maximums on the spectrum made by from the synthesized non-amidated KA_4. Each of these were collected and the vial containing the synthesized KA_4 were identified by freeze-drying each vial. Only the vial from maximum four contained peptide, this peptide was used for further experiments.

After these runs the HPLC program was changed to recognize maximums based on the absorbance at 205 nm instead of 220 nm.

3.4.2 Self-assembly

3.4.2.1 HPLC Purified

Figure 3.34A is an 5x5 μm AFM scan of an acidic sample of HPLC purified KA_4. Two different type of structures are visible on Figure 3.34A, rod-shaped structures on the left and structures with wide range of shapes and sizes on the right. The structures with varied shape has heights of 2-5 nm with an even surface. The rods have heights of 5-10 nm, diameters around 30 nm, and lengths down to 200 nm. Figure 3.34B is a zoom in to 1.5x1.5 μm and has a mixture of the two types of structures with some individual rods.

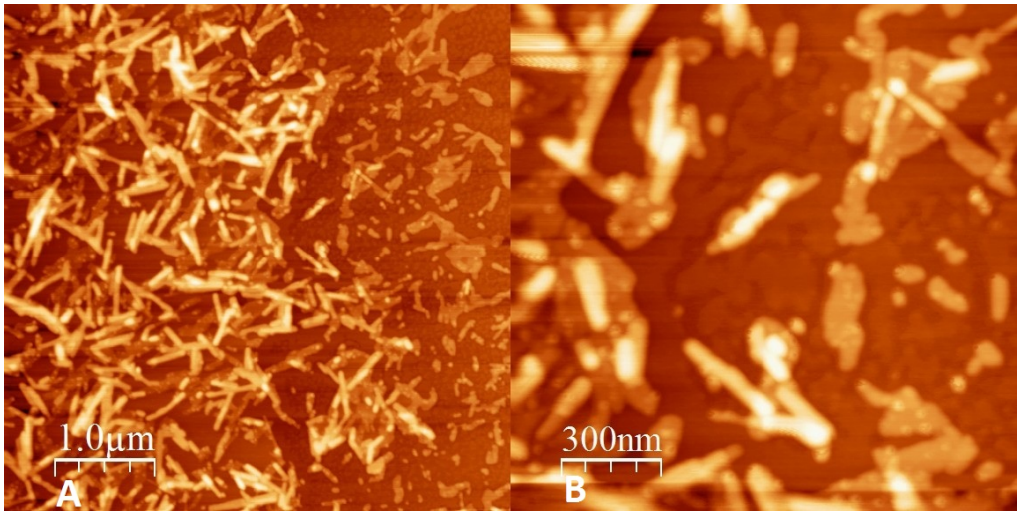

Figure 3.34: AFM scans of a mica surface where the HPLC purified KA_4, in an acidic solution, was immobilized. A is a scan area of 5x5 μm and B is 1.5x1.5 μm.

Figure 3.35 is AFM scans of a neutral solution of KA_4 immobilized on mica. Figure 3.35A is an 50x50 μm image of a wire with a diameter above 1 μm and a height around 50 nm. The wire has an area around it free from structures while the rest of the surface has a rough layer of structures with heights around 3 nm. Figure 3.35B is a zoom in of the wire to 5x5 μm, where it can be seen that the wire is not solid. Some structures are visible in the bottom right corner of the scanned area. These structures are rod-shaped and are around 3-5 nm high. An additional zoom in was done at the edge of the wire to 1.5x1.5 μm, Figure 3.35C. The wire seems to be formed from smaller rod-shaped structures.

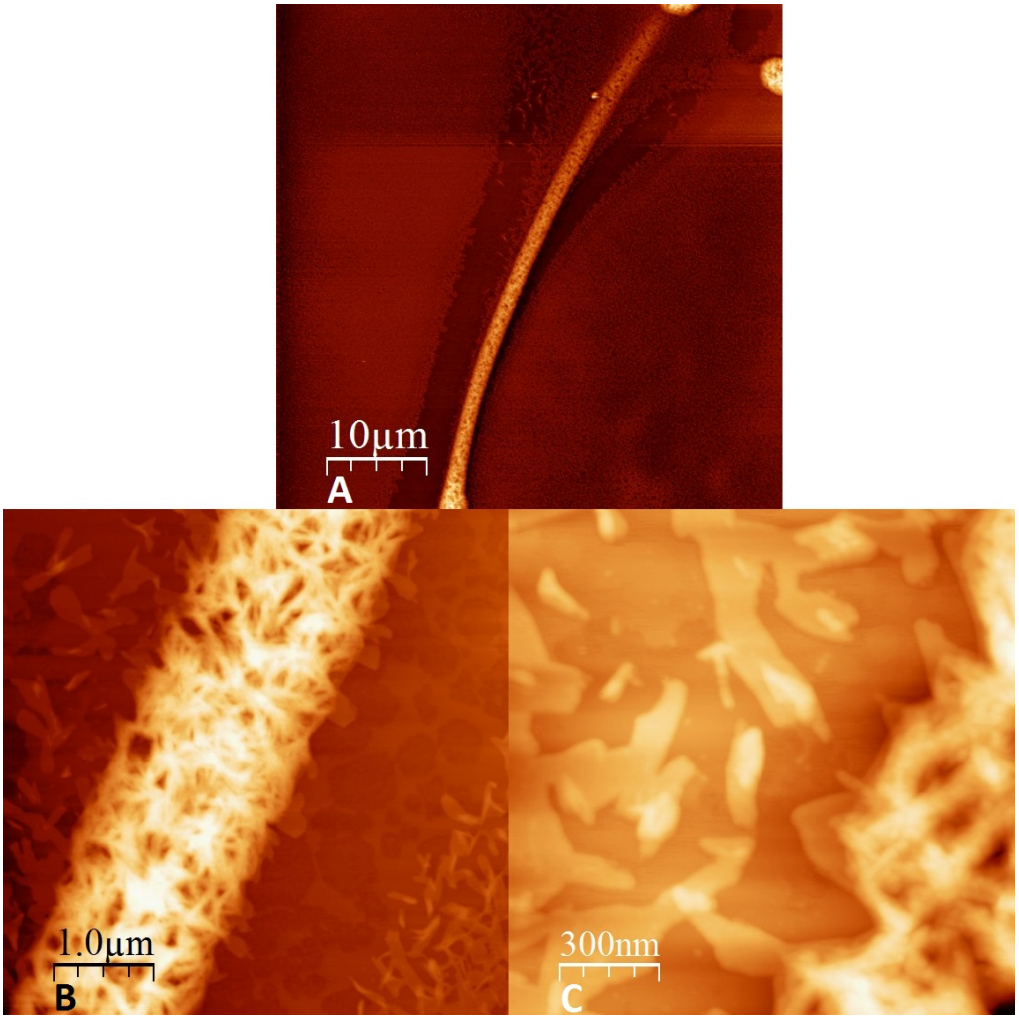

Figure 3.35: AFM scans of a mica surface where the HPLC purified KA_4, in an neutral solution, was immobilized. A is a scan area of 50x50 μm, B is 5x5 μm, and C is 1.5x1.5 μm.

Self-assembly were attempted with KA_4 in a basic solution, Figure 3.36. Figure 3.36A is a 5x5 μm scan of the mica surface where self-assembled KA_4 structures, formed in a basic solution, are immobilized. Two types of structures are present, one being a flat structure with height around 3 nm, This type of structure has a wide range of sizes and shapes. The second is an elipse-shaped structure with heights of around 10 nm, width around 100 nm, and length up to 300 nm. Figure 3.36B is a zoom in where both structures are present.

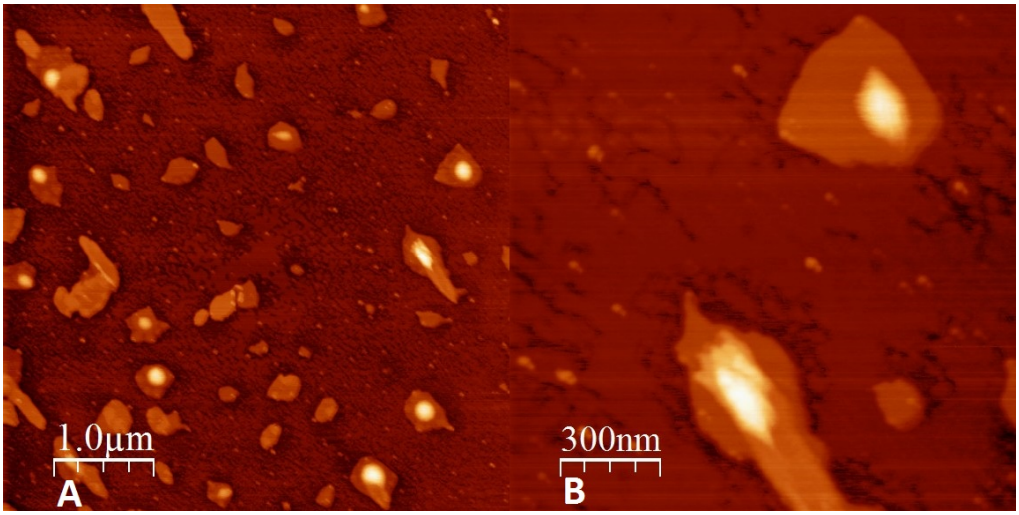

Figure 3.36: AFM scans of a mica surface where the HPLC purified KA_4, in an basic solution, was immobilized. A is 5x5 μm and B is 1.5x1.5 μm.

3.4.2.2 HCl Washed

The peptide was washed twice with 1 M HCl. The HCl washed peptide was used to make three solutions of KA_4, one acidic, one neutral, and one basic.

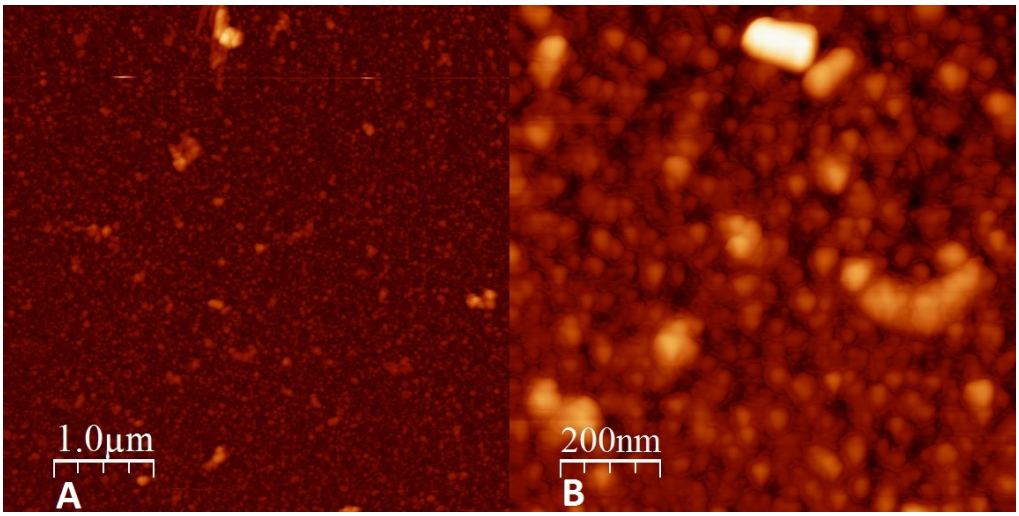

Figure 3.37: AFM scans of a mica surface where the HCl washed KA_4, in an acidic solution, was immobilized after one hour of self-assembly. A is a scan area of 5x5 μm and B is 1x1 μm.

The acidic solution of the HCl washed KA_4 was immobilized after one hour of self-assembly and imaged with AFM, Figure 3.37. Round structures are spread onto the entire 5x5 μm area that was scanned, Figure 3.37A. These round structures have heights of around 5-10 nm and diameters of around 20-40 nm, however some structures are larger with heights of around 100 nm and diameters of around 200 nm. Figure 3.37B is a zoom in of the structures to 1x1 μm.

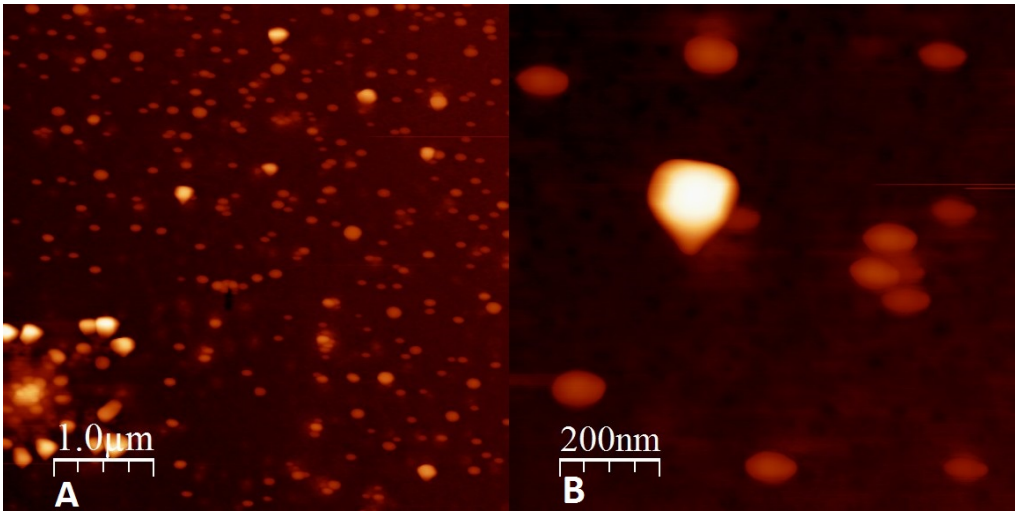

Figure 3.38: AFM scans of a mica surface where the HCl washed KA_4, in a neutral solution, was immobilized after one hour of self-assembly. A is a scan area of 5x5 μm and B is 1x1 μm.

Two types of structures are present on the scanned area of 5x5 μm, Figure 3.38A, of the neutral HCl washed KA_4. The first is a round structure with heights of around 15 nm and diameters between 50 and 100 nm. The second is a structure with sharper edges. The height of these structures are around 50 nm while the width is around 100-150 nm. Figure 3.38B is a zoom in to 1x1 μm where both types of structures are visible.

More than one type of structure is present on the 5x5 scan, Figure 3.39A, of the mica plate, where basic solution of HCl washed KA_4 was immobilized. The first is a rod-shaped structure with heights of around 20-30 nm, widths of around 100-150 nm, and lenghts of around 1-1.5 μm. The second type of structure is a round structure with heights of around 40 nm and diameters of around 200 nm. A third structure has height of around 2 nm and is spread onto the surface with various sizes and shapes.

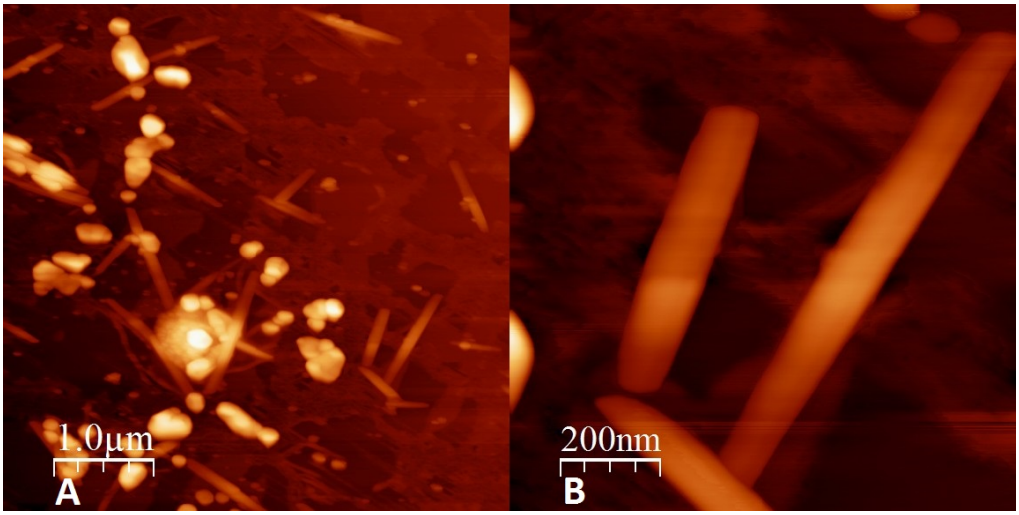

Figure 3.39: AFM scans of a mica surface where the HCl washed KA_4, in a basic solution, was immobilized after one hour of self-assembly. A is a scan area of 5x5 μm and B is 1x1 μm.

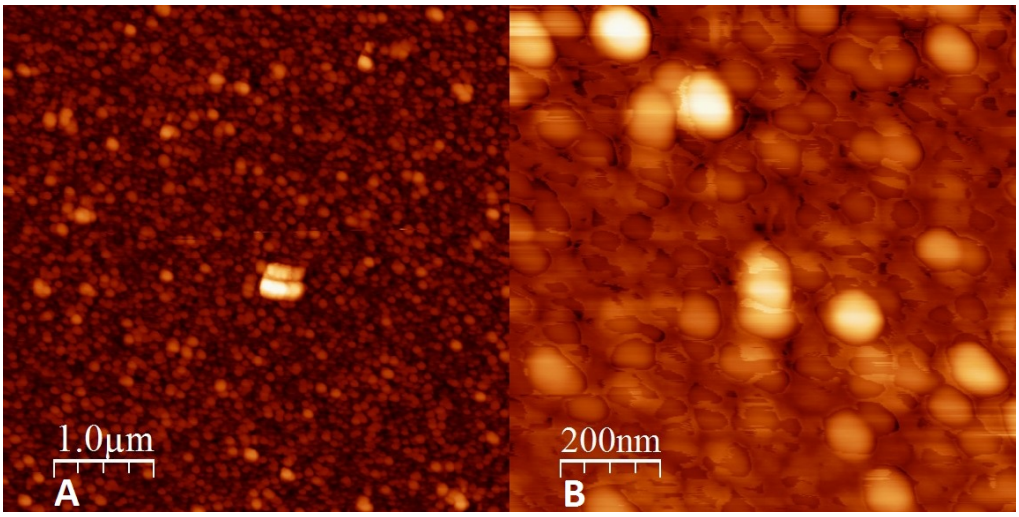

Figure 3.40: AFM scans of a mica surface where the HCl washed KA_4, in an acidic solution, was immobilized after 24 hours of self-assembly. A is a scan area of 5x5 μm and B is 1x1 μm.

The acidic solution of the HCl washed KA_4 was immobilized after 24 hours of self-assembly and imaged with AFM, Figure 3.40. Round structures are spread onto the entire 5x5 μm area that was scanned, Figure 3.40A. These round structures have heights around 10 nm and diameters around 50 nm, however some structures are larger with heights up to 60 nm and diameters of around 100 nm. Figure 3.37B is a zoom in of the structures to 1x1 μm.

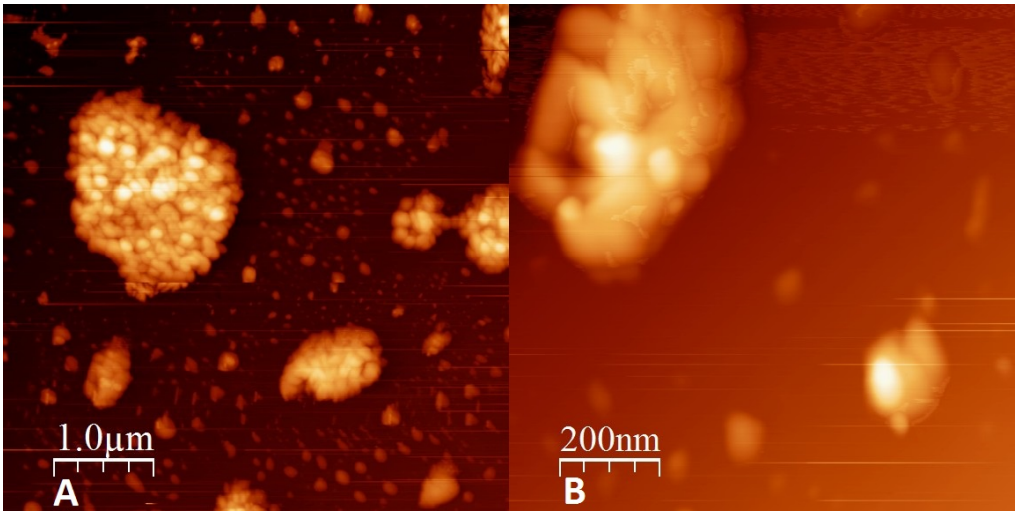

Figure 3.41: AFM scans of a mica surface where the HCl washed KA_4, in a neutral solution, was immobilized after 24 hours of self-assembly. A is a scan area of 5x5 μm and B is 1x1 μm.

The neutral solution of the HCl washed KA_4 was immobilized on mica after 24 hours of self-assembly. The mica surface with structures was imaged with AFM, Figure 3.41. Figure 3.41A is 5x5 μm scan of the surface, while Figure 3.41B is a 1x1 μm scan. Two types of structures are present, the first is individual round structures with heights of 5-10 nm and diameters of around 50-100 nm. The other type of structures are larger round structures with diameters up to 2 μm and height up to 80 nm. The larger structures could be aggregates of the smaller structures.

A sample from the basic solution of KA_4 was added to mica after 24 hours of self-assembly and scanned with AFM, Figure 3.42. More than one type of structure is seen, the first structure seen is rod-shaped structures with heights of 10-25 nm, widths of around 100-200 nm, and lenghts around 1 μm. The second type of structure is a round structure with heights of around 5 nm and diameters of around 40-60 nm. The last type of structure is a flat layer on the surface with height of around 2 nm.

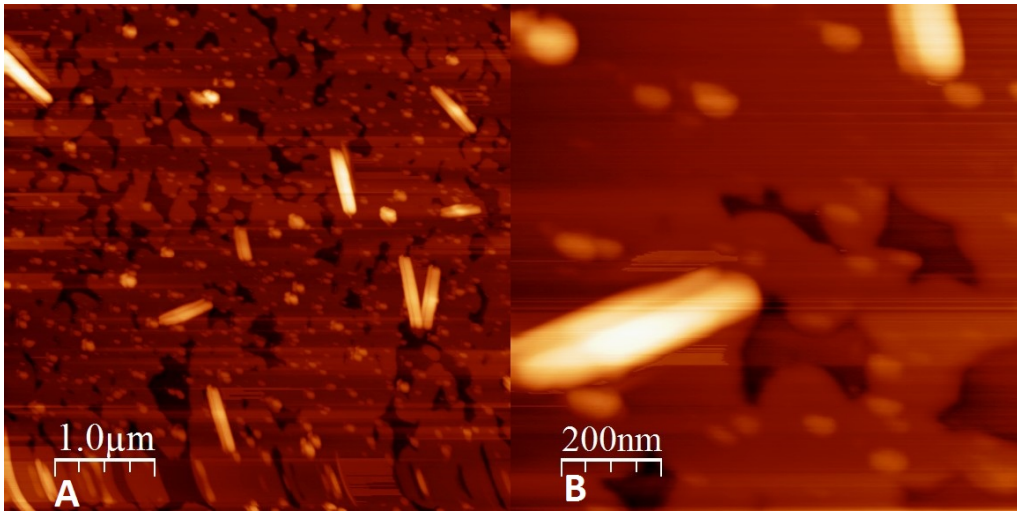

Figure 3.42: AFM scans of a mica surface where the HCl washed KA_4, in a basic solution, was immobilized after 24 hours of self-assembly. A is a scan area of 5x5 μm and B is 1x1 μm.

3.4.3 Thioflavin-T

A new solution of the HCl washed KA_4 was made investigate if structures seen with AFM were formed in solution or on the surface of mica, however due to the lack of peptide only neutral pH was investigated and the concentration of peptide was measured to around 9 mM.

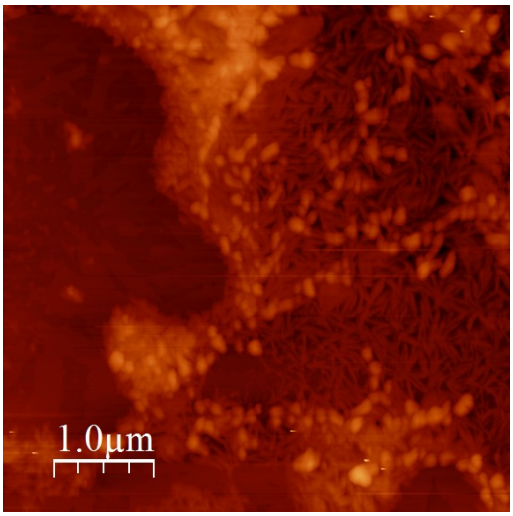

Figure 3.43: An AFM scan of a mica surface where the new solution of HCl washed KA_4 was immobilized after one hour of self-assembly. The scanned area is 5x5 μm.

A 5x5 μm area of the mica surface, where the new solution of KA_4 was immobilized, was scanned with AFM, Figure 3.43. Structures are seen on the surface. More than one type of structure is present, the first is a mesh of rod-shaped structures with heights of up to 10 nm. The second is a round structure with heights up to 50 nm and diameter up to 200 nm, however most have heights of around 25 nm and diameter around 100 nm. The last type of structure is a layer on the surface with height of around 2 nm and have various sizes and shapes.

A new control was made with pure thioflavin-T in water where polarized light was used. A polarizer was placed between the sample and the detector and two measurements were made, one where the polarizer was blocking the light used for excitation and one where the polarizer was open to the light used for excitation. These were compared and the results are illustrated by Figure 3.44A. The measured values was subtracted by the value measured with pure H_2O, illustrated by Figure 3.44B. The values increase from the start values of around 0.6 when the 0 μM measurement is subtracted and 0.4 when the 0 μM measurement is not subtracted. The values increase to being roughly stable around 1 at 5 μM when the 0 μM measurement is subtracted and to around 0.8 at 10 μM when the 0 μM is not subtracted.

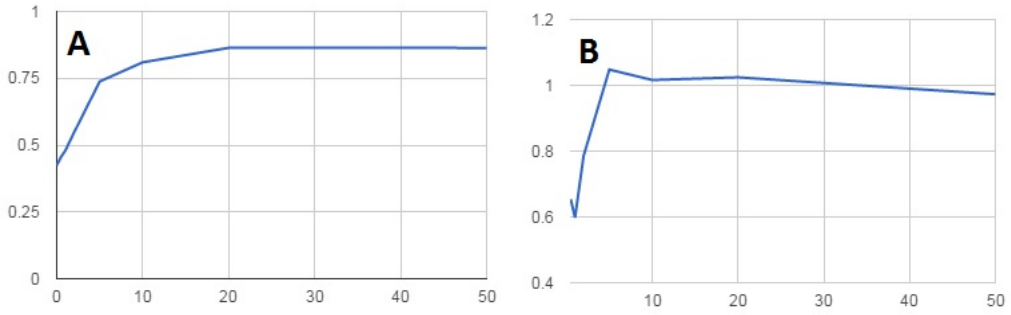

Figure 3.44: Illustration of the emission measured of thioflavin-T dissolved in H_2O. The first axis is the concentration of thioflavin-T and the second axis emission through the blocked polarizer divided by the emission through the open polarizer. A is made from measured values while B is the measured values from which the measurement from 0 μM thioflavin-T is subtracted.

The same procedure was used for samples containing ~9 mM KA_4 in solution at neutral pH and the results are illustrated by Figure 3.45. Figure 3.45A is the results when the measurement without thioflavion-T is not subtracted from the other measurements and Figure 3.45B is where the measurement without thioflavin-T is subtracted from the other measurements. The values for both sets of results are fluctuating at contrations of thioflavin-T below 10 μM. The value is stable around 0.8 at 10 μM to 20 μM thioflavin-T and increases to around 0.83 at 50 μM thioflavin-T when the measurement without thioflavin-T is not subtracted. The values are stable around 0.9 from 10 μM to 20 μM thioflavin-T and increases to around 1 at 50 μM thioflavin-T.

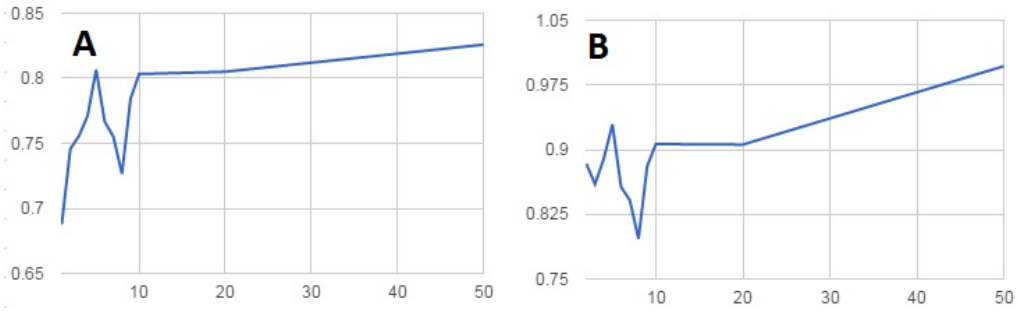

Figure 3.45: Illustration of the emission measured of thioflavin-T and KA_4 dissolved in H_2O. The first axis is the concentration of thioflavin-T and the second axis emission through the blocked polarizer divided by the emission through the open polarizer. A is made from measured values while B is the measured values from which the measurement from 0 μM thioflavin-T is subtracted.

After KA_4 were mixed with thioflavin-T, to a final concentration of 50 mM, another sample was immobilized on mica.

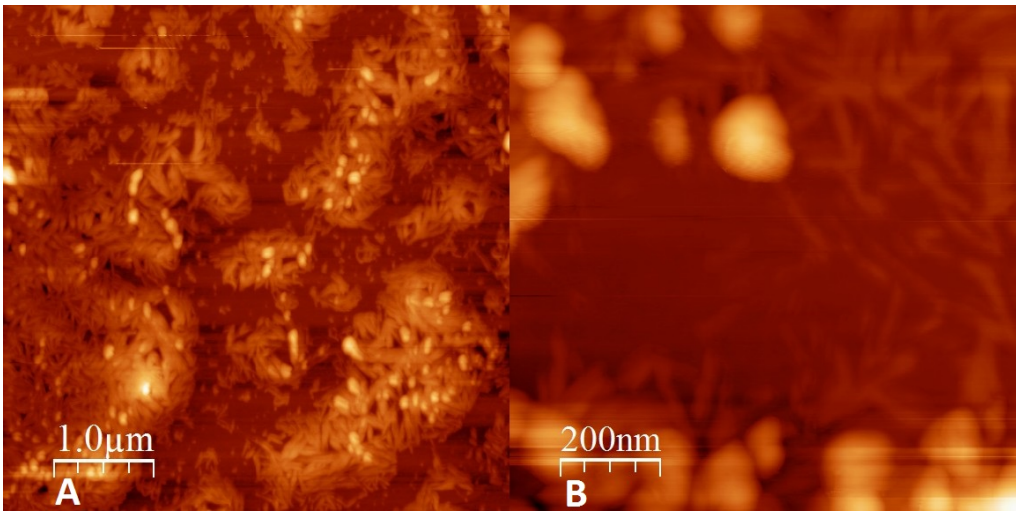

Figure 3.46: Two AFM scans of a mica surface where the new solution of HCl washed KA_4 was immobilized with 50 mM thioflavin-T. A has a scan area of 5x5 μm and B has a scan area of 1x1 μm.

Two AFM scans was made of KA_4, one has a scan area of 5x5 μm, Figure 3.46A, the other is a zoom in to a scan area of 1x1 μm, Figure 3.46B. Two types of structures are present, one being a rod-shaped structure with heights of around 4 nm and widths of 40 nm. The other is round structures with heights of around 25 nm and diameters around 100 nm.
The structures before and after the addition of thioflavin-T are similar.

3.4.4 In Silico

An in silico experiment was done with 50 KA_4 in a 5x5x5 nm box. The result of the experiment is a rod-shaped structure where the ends are wider than the center. The diameter of the center is around 2 nm while ends are around 3 nm in one direction and the full width of the box, 5 nm, in the other direction. The lenght of the wire is the full length of the box. The structure is illustrated by Figure 3.47.

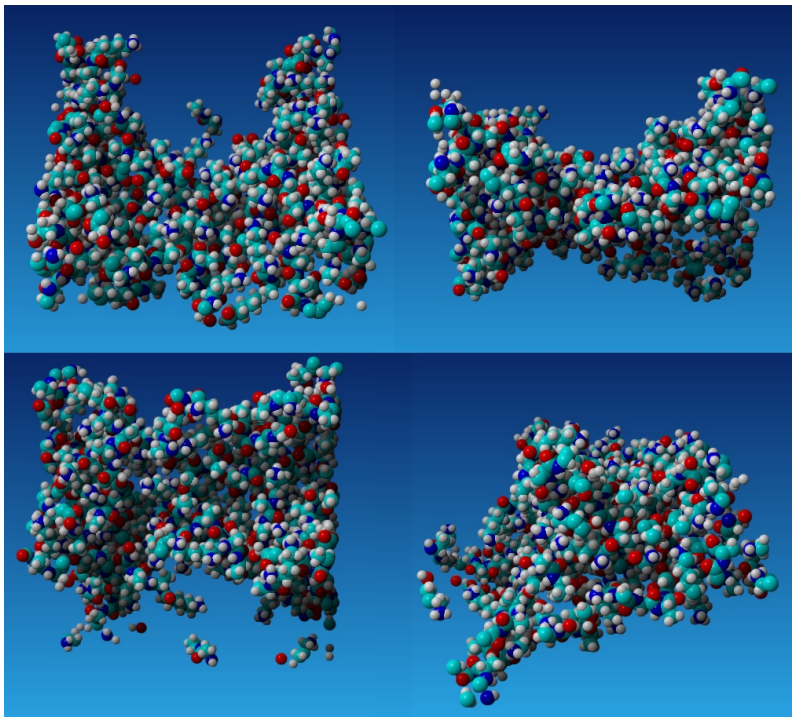

Figure 3.47: The result from the in silico experiment with 50 KA_4 in a 5x5x5 nm box visualized from four directions.

CHAPTER 4

DISCUSSION

All four peptides were synthesized through solid-phase peptide synthesis. However the two of the synthesis were interrupted for unknown reasons. The synthesis of KA_4 was interrupted at the third alanine and the synthesis of KA_6 was interrupted at the fourth alanine. Both synthesis were continued the next morning. The peptides were cleaved from the resin with success, however the effectiveness of the cleave was not investigated.

The HPLC runs indicates that by-products were synthesized with the peptides since a lot of maximums were recognized by the program and collected. The HPLC programs were optimized during the runs done. Even with the optimized HPLC programs for the later runs, a high amount of signals were still found and collected. The initial program was changed due to the peptides leaving the columns too early. A control run with 0.1% TFA dissolved in H_2O through the large column, Figure 3.2A, has maximums between minute two and minute four, however the sample of KA_5 has no maximums before minute four. Since the peptide is leaving the column early in the run it could contain these contaminants. The contaminants could have been investigated with mass spectroscopy to determine what contaminants were present if any. When the program was changed and a sample was run, Figure 3.20B, where the peptide exits the column after the potential contaminants. Therefore KA_5 may not be free from contaminants even though the peptide was HPLC purified.

It was attempted to determine the concentrations of non-amidated KA_5. A theoretical concentration of around 10 mM KA_5 in H_2O was made and absorbance was measured and the solution were diluted to measure an absorbance below 2. The absorbance of the peptide solution was saturated, above 2 when the peptide solution was diluted 500 times. This gives a concentration of at least 50 mM, which is five times more than the mass added would allow. This is most likely caused by contaminants that absorbs at 205 nm. Therefore concentrations are not noted for KA_5. This is also the reason why the concentration of KA_4 and KA_6 were not attempted to determine before new solution were made.

Since contaminants are most likely present in the solution of KA_5, they may have had an influence on which structures were formed during self-assembly. Furthermore if enough contaminants are present the concentration of peptide may be lower than the CMC of the peptide. This could lead to that no structures are self-assembling in the solution.
If no structures are formed in the solution it could lead to a layer of peptide on mica as seen with the neutral peptide solution of amidated KA_5, Figure 3.4, that has a layer with height of around 1 nm, this suits the height of a monolayer. Another type of layer is the rough layer on the basic sample of the HCl washed non-amidated KA_5, Figure 3.10C, this layer have a height of around 2 nm, that is similar to the height of a bilayer.

No structures in the solutions may also lead to structures being formed on the surface of mica, during the immobilization of the potential structures. The concentration in the droplet on mica may have local concentrations higher than CMC while drying, which would allow for structures to self-assembly. The drying of the droplet may also change the structures already present in the solution and allow for further self-assembly, and thereby changing the structures in the solution. Further self-assembly on mica could be the reason behind the structures formed with the HPLC purified KA_4 in neutral solution, Figure fig:14. Individual wires may have formed in the solution and during the drying the local concentrations of wires allowed for a high amount of structure to be deposited in certain locations.
The drying of the droplet may also allow for the formation of large aggregates instead of self-assembled structures.

It was attempted to remove some leftovers that could bind to the peptides, from the synthesis and the HPLC purification, e.g. TFA, by washing the peptide with 1 M HCl. Leftover TFA could potentially form a bond to the N-terminus of the peptide and thereby affecting the self-assembling properties of the peptide. However crystals are present after the HCl wash, which indicates the presence of a salt. An example of an AFM scan where crystals are present is the acidic solution of HCl washed non-amidated KA_5, Figure 3.10A. Which salt is present and if the removal of TFA was successful could have been investigated with mass spectroscopy.

It was investigated if the structures seen during the AFM scans were formed in the solution or on the surface of mica. During this experiment thioflavin-T was added to the solution. Thioflavin-T could change the structures formed and change the CMC of the structures, this could lead to new structures being formed or current structures being dissolved. Therefore the structures seen with AFM after the addition of thioflavin-T might not be the same as the structures in the solution, if any, before thioflavin-T was added.
The structures seen with AFM of non-amidated KA_4 before, Figure 3.43, and after, Figure 3.46, the addition of thioflavin-T were very similar and the same types of structures were present. Thioflavin-T does not seem to change the structures self-assembled by KA_4.

Two detectors were used during the experiment with thioflavin-T. With thioflavin-T dissolved in H_2O without peptide the emission of one detector was fluctuating below 5 μM, however the other detector measured a steady increase from 0.5 μM until the max emission at

20 μM.

4.1 In Silico Experiments

Two in silico experiment were run for around 60 ns. One experiment was done with 25 non-amidated KA_5 dissolved in H_2O in a 5x5x5 nm box, and the other was done with 25 non-amidated KA_4 dissolved in H_2O, however no change was seen in either experiment during the 60 ns. The water was removed and the experiment was restarted with 50 peptides. This may have caused the in silico experiments to produce structures that would not be formed if the experiments were run in H_2O.

All in silico results were obtained with 50 peptides in a 5x5x5 nm box with periodic cell boundaries. This yielded the concentration of peptide to be greatly increased compared to the concentration during the in vitro experiments. This may have caused the in silico experiment to produce another structure than the in vitro experiment, solely based on the concentration of the peptides.

The in silico experiments were run between 25 and 70 ns and the structures produced may not be the final state of equilibrium, other structures may have formed if the experiments were run for longer.

4.2 KA_5

The amidated KA_5 at neutral pH was found to form a layer with height of around 1 nm, however this was before the HCl wash and therefore leftovers from the synthesis that could impact the self-assembling properties. Due to this no in silico experiment was done with amidated KA_5.

In silico experiments were made with the non-amidated KA_5, and the in silico experiment suggests that the structures formed by non-amidated KA_5 through self-assembled would be a wire or a rod-shaped structure, Figure 3.18. This corresponds with some of the in vitro experiments. Wires were formed by the non-amidated KA_5, Figure 3.7 and Figure 3.8, before the HCl wash. The heights of the produced wires were around 3-5 nm and the wires had widths around 25 nm, which the in silico wire did not. The wire produced in silico had a diameter of 3 nm which corresponds with the height but not the width of the produced wire. Other wires with similar height were produced in vitro after the HCl wash and while the solution. In the neutral solution wires with height of 4 nm were formed, Figure 3.15, and in the basic solution wires with heights of around 6 nm were formed, Figure 3.16, after one hour of self-assembly. However no in vitro experiment fits the wire width of the in silico experiment. All the wires produced in vitro were among other structures.

It was investigated if the structures visualized with AFM were formed in solution or were

formed on the surface of mica. The emission of thioflavin-T dissolved in H_2O, Figure 3.11, was compared to the emission of thioflavin-T and KA_5 dissolved in H_2O, Figure 3.13. Both detectors when the solution is without peptide has a max value at 20 μM thioflavin-T. However the solutions with peptide KA_5 has a steeper ascent towards the maximum emission, and the second detector reached the maximum emission when the concentration of thioflavin-T was 10μM and not the 20 μM thioflavin-T as the solution without any peptide. The only substance in the solution that could cause these changes is structures formed by KA_5 that could bind thioflavin-T.

4.3 KA_6

In silico experiments were made with the non-amidated KA_6, which suggests that the structures formed by KA_6 are layers with height of around 2-3 nm. No layers were formed during the in vitro experiments, however flat structures were observed on the AFM scan of the basic solution of KA_6 after 24 hours of self-assembly, Figure 3.29. This structure has heights of around 2-3 nm and widths between 50 and 100 nm, however the width and shape of these structures vary. A similar structure is seen in the same solution but after one hour of self-assembly, Figure 3.26, these structures have height of around 5 nm.

In vitro experiments on KA_6 were done by Gurevich et al. in 2010 [7]. They found that KA_6 formed similar structures at basic and neutral pH, a rod-shaped structure, while forming micelles at basic pH. [7] This is only partly consistent to the in vitro experiments, where it was found that KA_6 at acidic and neutral pH formed similar structures. However the structures formed in acidic, Figure 3.27, and neutral, Figure 3.28, solution were round structures, while the structures formed in basic, Figure 3.29, solution were rod-shaped.

Experiments with A_6K were done by Colherinhas et al. in 2014. [15] They found that A_6K formed nanotubes with an inner diameter of 1.5 nm and an outer diameter of 4.9 nm, through in silico experiments. Through in vitro Colherinhas et al. found that A_6K formed tubes with diameter of around 5 nm. The diameter of the tubes created by Colherinhas et al. are similar to the height of the rod-shaped structures found with KA_6 in basic solution after one hour of self-assembly, Figure 3.23. However the experiments might not be perfect comparable since the lysine in the experiment of Colherinhas et al. was at the C-terminus and not the N-terminus. [15]

The reason behind the inconsistencies could be that the KA_6 that was used for in vitro experiments was not completely pure. The solution made for experiments with thioflavin-T was unclear and had solid residues after the solution was left at 5°C for a few days. The fluorescence of the solution was measured and the solution was fluorescent at a wide range of wavelengths, including the wavelengths where the fluorescence of thioflavin-T would have been measured. These impurities could affect the self-assembling properties of KA_6 and thereby making the in vitro experiments inconsistent with the experiments done by Gurevich et al. in 2010 and the in silico experiments.

4.4 KA_4

In silico experiments were made with the non-amidated KA_4, which suggests that the structures formed by KA_4 are wires with diameter of 2 nm. No rod-shaped structure with that size were observed during the in vitro experiments with KA_4, however other rod-shaped structures were observed. An example of these rod-shaped structures are the structures formed by KA_4 in acidic solution after the HPLC purification, Figure 3.34, and the neutral solution after the HPLC purification, Figure 3.35. The rods in the acidic solution have heights from 3 nm while the rods in the neutral solution have heights from 5 nm.
Structures with height of around 2 nm has also been observed during the in vitro experiments with KA_4. These structures were not rod-shaped, but layers. An example of these layers is the layer formed by the HCl washed KA_4 in basic solution after 24 hours of self-assembly, Figure 3.42.

It was investigated if the structures visualized with AFM were formed in solution or were formed on the surface of mica. The ratio between the detected emissions through the blocked and the open polarizer were compared. The fluctuating values from the solution with KA_4, Figure 3.45, makes the two experiments hard to compare, since the low concentrations of thioflavin-T with KA_4 was affected by noise. All measurements had an increase in this ratio with higher concentration of thioflavin-T. This would mean that thioflavin-T is more free to move and rotate when the concentration is high than when the concentration is low which is counter intuitive. It would be expected that when micelles of thioflavin-T are formed the individual molecules would move less in the solution than if the molecules are dissolved in H_2O without the formation of structures.

The emissions from the experiment without KA_4 where the emission of 0 μM has been subtracted from the remaining emissions has values around 1 from the measurement with 5 μM thioflavin-T, which is the CMC of thioflavin-T [16]. This would suggest that the individual molecules of thioflavin-T are free to move when the concentration is above CMC.

4.5 A_6K as a Potiential Delivery System

Many important hydrophobic drugs exists in medicine e.g. doxorubicin and paclitaxel used for chemotherapy in cancer treatment. These drugs are effective but they have low solubility in water. Because of the low solubility of the hydrophobic drugs, a high amount of research is done aiming to increase the solubility, by creating simple structures that can enclose drugs. [17] [18]

Chen et al. attempted to increase the solubility of the model drug pyrene by using A_6K as a drug carrier, and thereby found a potential carrier and delivery system for hydrophobic drugs. It was found that A_6K was able to encapsulate pyrene in two different ways. The first way was that the hydrophobic center of the micellar nanofibers trapped pyrene, while the second way was that pyrene would be wrapped by nanofibers and form nano crystals. Both ways increased the solubility of pyrene in water. Furthermore it was found that pyrene could

be released with ease. [17]
It is suggested that the delivery system could be modified to have targeted delivery and thereby using surfactant-like peptides as a drug delivery system.[17] It may also be possible to design a structure for drug-delivery that allows for slowly release of both hydrophobic and hydrophilic drugs. [19]

4.6 Surfactant-like Peptide Nanofiber Complexes with siRNA

Traditional treatments for the central nervous system disorders are, in many cases, not selective, since drugs with small molecular weight can cross the barrier between blood and brain. One approach for switching off specific genes could be an interference of RNA of genes involved in illness. This process should be able to target specific genes in specific brain cells and therefore should be highly selective. This is currently hard to achieve. siRNA are not able to pass through cell membranes, and needs to be transported into the cytoplasm before they can silence a RNA. Many carriers used today are, lipid, polymer, carbon, or inorganic nanoparticles. [20]

Mazza et al. [20] attempted to use peptide nanofibers as carriers for siRNA. The peptide nanofibers used were self-assembled from surfactant-like peptides. The peptides used were palmitoyl-GGGAAAKRK with a hydrophobic tail consisting of palmitoyl covalently bound to the N-terminus, three positively charged amino acids as headgroup, and a center consisting of six amino acids that form a β-sheet. The positively charged headgroups leads to the nanofibers having a positively charged surface and thereby form stronger bounds to the slightly negatively charged siRNA. [20]
It was found that peptide nanofibrils can form complexes with siRNA and thereby the peptide nanofibrils can be used as intracellular transport, both in vitro and in vivo. It was also found that the biological activity of the siRNA was maintained and lead to decreased protein levels. [20]

4.7 Surfactant-like Peptides Drive Soluble Proteins into Active Aggregates

During expression of heterologous proteins produced in a recombinant host, e.g. *E. coli*, the proteins can be overexpressed and thereby may form inactive inclusion bodies. This can lead to a high amount of protein that has no way to be recovered through refolding. [21]

The possibility of forming aggregates that retain the activity of native protein was investigated by Zhou et al. in 2012. [21] With model proteins it was shown that by attaching surfactant-like peptides, like L_6KD, L_6K_2, and DKL_6, to a soluble protein can cause the proteins to form active aggregates, and thereby keeping some of the activity of the native protein. It was reported that the active aggregates maintained from 25% to 92% activity of their native counterparts. It was observed that uncharged hydrophilic headgroups were better at maintaining the activity of the proteins, while the position of the headgroups made less of

a change. It was suggested that the findings could find uses in e.g. protein purification and for biocatalysts. [21]

4.8 Antibacterial and Antitumor Surfactant-like Peptides

Antibacterial peptides are candidates for future antibiotics even though antibacterial peptides work in a different way than current antibiotics. Current antibiotics target specific receptors on e.g. a bacteria where antibacterial peptides would target the cell membrane. Natural occurring antibacterial peptides have similarities e.g. having a positive charge and being amphiphilic. The positive charge allows for easier binding to the negatively charged surface of a bacteria and the amphiphilic properties allows the peptide to disturb the membrane. Some of the antibacterial peptides even show toxicity towards tumor cells. [22]

Chen et al. [22] investigated the antibacterial properties of surfactant-like peptides, A_9K, A_12K, and A_9K_2, and it was found that peptides can kill both bacterial and tumor cells. It was also found that the peptides had a high level of selectivity and was friendly towards host mammalian cells, which is crucial for development of anticancer peptides. Experiments were done with both mouse embryo cells and red blood cells, in both cases the peptides left the host cells unharmed, while causing lysis to the bacteria cells and tumor cells. It was suggest that surfactant-like peptides via peptide design and optimization could be useful in biomedicine. [22] [23]
Xu et al. reported that A_9K inhibits cell growth of HeLa in two ways. The first being disruption of the cell membranes and the second being mitochondria dependent cell apoptsis. [23]
The antibacterial effect of surfactant-like peptides was also reported by Dehsorkhi et al. [24], who investigated A_6R. It was reported that A_6R interacted with lipid membranes and thereby exhibit antimicrobial activity, however no activity towards tumor cells were reported. [24]

CHAPTER 5

CONCLUSION

Studies were made on the self-assembling properties of surfactant-like peptides. Peptides of the KA_5 family were synthesized using solid-phase peptide synthesis. After the synthesis the peptides were purified through HPLC. Self-assembly was attempted with the peptides in an acidic, a neutral, and a basic solution. It was found that the peptide solutions still contained salt and traces of trifluoroacetic acid and therefore a wash with HCl were done. The structures formed by the surfactant-like peptides were investigated with atomic force microscopy. The hydrophobic dye thioflavin-T was used in an attempt to determine if the structures were formed in solution or on the surface of mica. It was determined that the structures of non-amidated KA_5 was formed in solution and not on the surface of mica. In silico experiments were done and the structures were compared to the structures found in vitro, and some similarities were found. The structures formed by KA_6 were compared to structures suggested by literature. Both KA_4 and KA_6 were found to contain contaminants e.g. salt.

BIBLIOGRAPHY

[1] Honggang Cui, Matthew J. Webber, Samuel I. Stupp. Self-Assembly of Peptide Amphiphiles: From Molecules to Nanostructures to Biomaterials. *Peptide Science*, Vol. 94, 2009.

[2] Ju Liang, Wen-Lan Wu, Xiao-Ding Xu, Ren-Xi Zhuo, Xian-Zheng Zhang. ph responsive micelle self-assembled from a new amphiphilic peptide as anti-tumor drug carrier. *Colloids and Surfaces B:Biointerfaces*, Vol. 114:398–403, 2014.

[3] I. W. Hamley. Self-assembly of amphiphilic peptides. *Soft Matter*, Vol. 7:4122–4138, 2011.

[4] Chengkang Tang, Feng Qiu, Xiaojun Zhao. Molecular design and applications of self-assembling surfactant-like peptides. *Journal of Nanomaterials*, 2013.

[5] Jacob N. Israelachvili. *Intermolecular and Surface Forces*. Academic Press, 2nd edition, 1992. ISBN-10: 0123751810, chapter 16-17.

[6] Steve J. Yang and Shuguang Zhang. Self-assembling Behavior of Designer Lipid-like Peptides. *Supramolecular Chemistry*, Vol. 18:389–396, 2006.

[7] Leonid Gurevich, Trine Wrist Poulsen, Ole Zoffmann Andersen, Nikolaj Lillelund Kildeby, and Peter Fojan. pH-dependent self-assembly of the short surfactant-like peptide KA_6. *Journal of Nanoscience and Nanotechnology*, Vol. 10:1–5, 2010.

[8] Sylvain Vauthey, Steve Santoso, Haiyan Gong, Nicki Watson, and Shuguang Zhang. Molecular self-assembly of surfactant-like peptides to form nanotubes and nanovesicles. *Proceedings of the National Academy of Science of the United States of America*, Vol. 99:5355–5360, 2002.

[9] Jacob N. Israelachvili, D. John Mitchell, and Barry W. Ninham. Theory of self-assembly of hydrocarbon amphiphiles into micelles and bilayers. *Journal of the Chemical Society, Faraday Transactions 2: Molecular and Chemical Physics*, Vol. 72:1525–1568, 1976.

[10] Xiaojun Zhao and Shuguang Zhang. Molecular designer self-assembling peptides. *Chemical Society Reviews*, Vol. 35:1105–1110, 2006.

[11] Steve Santoso, Wonmuk Hwang, Hyman Hartman, and Shuguang Zhang. Self-assembly of surfactant-like peptides with variable glycine tails to form nanotubes and nanovesicles. *Nano Letters*, Vol. 2, No. 7:687–691, 2002.

[12] Knud J. Jensen, Pernille Tofteng Shelton, and Søren L. Pedersen. *Peptide Synhtesis and Applications*. Humana Press, 2nd edition, 2013. ISBN 978-1-62703-543-9.

[13] Andrew R. Leach. *Molecular Modelling Principles and Applications*. Prentice Hall, 2nd edition, 2001. ISBN-10: 0582382106, chapter 4.

[14] Nicholas J. Anthis and G. Marius Clore. Sequence-specific determination of protein and peptide concentrations by absorbance at 205 nm. *Protein Science*, Vol. 22:851–858, 2013.

[15] Guilherme Colherinhas and Eudes Fileti. Molecular Dynamics Study of Surfactant-Like Peptide Based Nanostructures. *The Journal of Physical Chemistry B*, Vol. 118:12215–12222, 2014.

[16] Ritu Khurana, Chris Coleman, Cristian Ionescu-Zanetti, Sue A. Carter, Vinay Krishna, Rajesh K. Grover, Raja Roy, Shashi Singh. Mechanism of thioflavin T binding to amyloid fibrils. *Journal of Structural Biology*, Vol. 151:229–238, 2005.

[17] Yongzhu Chen, Chengkang Tang, Jie Zhang, Meng Gong, Bo Su, Feng Qiu. Self-assembling surfactant-like peptide A_6K as potential delivery system for hydrophobic drugs. *International Journal of Nanomedicine*, Vol. 10:847–858, 2015.

[18] Shuguang Zhang. Lipid-like Self-assembling Peptides. *Accounts of Chemical Research*, Vol. 45:2142–2150, 2012.

[19] Dimitrios G. Fatouros, Dimitrios A. Lamprou, Andrew J. Urquhart, Spyros N Yannopoulos, Ioannis S. Vizirianakis, Shuguang Zhang, and Sotirios Koutsopoulos. Lipid-like Self-assembling Peptide Nanovesicles for Drug Delivery. *Applied Materials and Interfaces*, Vol. 6:8184–8189, 2014.

[20] Mariarosa Mazza, Marilena Hadjidemetriou, Irene de Lázaro, Cyrill Bussy, and Kostas Kostarelos. Peptide Nanofiber Complexes with siRNA for Deep Brain Gene Silencing by Stereotactic Neurosurgery. *American Chemical Society*, Vol. 9:1137–1149, 2015.

[21] Bihong Zhou, Lei Xing, Wei Wu, Xian-En Zhang, and Zhanglin Lin. Small surfactant-like peptides can drive soluble proteins into active aggregates. *Microbial Cell Factories*, Vol. 11, 2012.

[22] Cuixia Chen, Jing Hu, Shengzhong Zhang, Peng Zhou, Xichen Zhao, Hai Xu, Xiubo Zhao, Mohammed Yaseen, and Jian R. Lu. Molecular mechanisms of antibacterial and antitumor actions of designed surfactant-like peptides. *Biomaterials*, Vol. 33:592–603, 2012.

[23] Hai Xu, Cui Xia Chen, Jing Hu, Peng Zhou, Ping Zeng, Chang Hai Cao, Jian Ren Lu. Dual modes of antitumor action of an amphiphilic peptide A_9K. *Biomaterials*, Vol. 34:2731–2737, 2013.

[24] Ashkan Dehsorkhi, Valeria Castelletto, and Ian W. Hamley. Interaction between a Cationic Surfactant-like Peptide and Lipid Vesicles and Its Relationship to Antimicrobial Activity. *American Chemical Society*, Vol. 29:14246–14253, 2013.

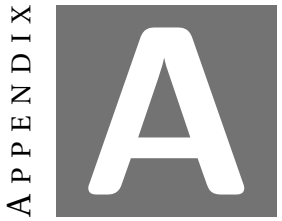

APPENDIX

A.1 Thioflavin-T Data

The data collected during the experiments with Thioflavin-T and peptide.

Concentration μM	Detector one	Detector two
50	9137.6	14590.5
20	10203	15465.2
10	8082.82	14194.2
5	7575.16	12915.1
2	8425.42	12226.1
1	6779.93	11979
0.5	8144.2	11355.1
0	7072.11	10905.8

Table A.1: The emissions of Thioflavin-T dissolved in H_2O measured by two detectors.

Concentration μM	Detector one	Detector two
0	9326.3	13869.6
0.5	10832.1	15740.8
1	10845.5	17205.7
2	11705	18458.6
5	13211.6	21148.7
10	14214.4	23463.4
20	15362.2	23319.5
50	15156.1	22372.6

Table A.2: The emissions of Thioflavin-T and KA_5 dissolved in H_2O measured by two detectors.

Concentration μM	Blocked	Open
0	77.7794	183.342
0.5	96.6692	212.234
1	128.893	268.909
2	151.117	276.687
5	272.242	368.925
10	425.604	525.629
20	592.315	685.68
50	795.723	921.339

Table A.3: The emission of Thioflavin-T dissolved in H_2O measured by one detector. The light used for excitation was polarized and the measured was through a polarizer blocking or allowing the original polarization.

Concentration μM	Blocked	Open
0	536.743	951.354
0.5	912.443	1453.89
1	1294.89	1883.16
2	1644.05	2204.62
3	2035.54	2694.15
4	2019.97	2619.59
5	2282.49	2829.9
6	2371.49	3093.64
7	2309.19	3058.03
8	2290.28	3152.63
9	2453.82	3128.15
10	2536.15	3157.08
20	2596.23	3224.98
50	1988.83	2408.2

Table A.4: The emission of Thioflavin-T and KA_4 dissolved in H_2O measured by one detector. The light used for excitation was polarized and the measured was through a polarizer blocking or allowing the original polarization.